J. Fluid Mech. (1997), *vol.* 340, *pp.* 361–394. Printed in the United Kingdom

On the nonlinear evolution of a pair of oblique Tollmien–Schlichting waves in boundary layers

By XUESONG WU[1], S. J. LEIB[2] AND M. E. GOLDSTEIN[3]

[1]Department of Mathematics, Imperial College, 180 Queens Gate, London SW7 2BZ, UK
[2]NYMA Inc., Lewis Research Center Group, Cleveland, OH 44135, USA
[3]Lewis Research Center, Cleveland, OH 44135, USA

(Received 1 August 1996 and in revised form 14 February 1997)

This paper is concerned with the nonlinear interaction and development of a pair of oblique Tollmien–Schlichting waves which travel with equal but opposite angles to the free stream in a boundary layer. Our approach is based on high-Reynolds-number asymptotic methods. The so-called 'upper-branch' scaling is adopted so that there exists a well-defined critical layer, i.e. a thin region surrounding the level at which the basic flow velocity equals the phase velocity of the waves. We show that following the initial linear growth, the disturbance evolves through several distinct nonlinear stages. In the first of these, nonlinearity only affects the phase angle of the amplitude of the disturbance, causing rapid wavelength shortening, while the modulus of the amplitude still grows exponentially as in the linear regime. The second stage starts when the wavelength shortening produces a back reaction on the development of the modulus. The phase angle and the modulus then evolve on different spatial scales, and are governed by two coupled nonlinear equations. The solution to these equations develops a singularity at a finite distance downstream. As a result, the disturbance enters the third stage in which it evolves over a faster spatial scale, and the critical layer becomes both non-equilibrium and viscous in nature, in contrast to the two previous stages, where the critical layer is in equilibrium and purely viscosity dominated. In this stage, the development is governed by an amplitude equation with the same nonlinear term as that derived by Wu, Lee & Cowley (1993) for the interaction between a pair of Rayleigh waves. The solution develops a new singularity, leading to the fourth stage where the flow is governed by the fully nonlinear three-dimensional inviscid triple-deck equations. It is suggested that the stages of evolution revealed here may characterize the so-called 'oblique breakdown' in a boundary layer. A discussion of the extension of the analysis to include the resonant-triad interaction is given.

1. Introduction

Laminar–turbulent transition in an incompressible flat-plate boundary layer usually involves a predominantly two-dimensional linear stage, followed by a three-dimensional stage in which nonlinear effects become significant. Since turbulence can be sustained only when it is three-dimensional (if there is no external force), the latter stage is of fundamental importance for understanding transition to turbulence.

The initial development of three-dimensional effects is often due to a resonant interaction between a two-dimensional fundamental disturbance and a pair of oblique instability waves, with equal but opposite spanwise wavenumbers. The resonance can cause the oblique waves to become large enough to interact with themselves so that the dominant nonlinear activity becomes the self-interaction between a pair of oblique Tollmien–Schlichting (T-S) waves. Certain flow structures, such as streamwise vortices and high-shear layers, which are believed to be crucial for the generation of small-scale turbulence, have been attributed to such an interaction. Alternatively, transition can also be induced by directly introducing a pair of oblique T-S modes into the flow, bypassing the initial two-dimensional stage. This is the so-called oblique-mode breakdown.

A completely self-consistent theoretical analysis of such processes can strictly be carried out only in the context of a high-Reynolds-number asymptotic approach. Such an approach allows the systematic inclusion of nonlinear, non-parallel etc. effects.

In incompressible boundary layers, the linear instability wave growth rate in the majority of the unstable range is small compared with its wavelength. As such, the initial nonlinear interactions will occur in the critical layer surrounding the transverse position where the mean flow velocity is equal to the phase speed. Even in more unstable flows viscous spreading of the mean flow can often cause the growth rate to be relatively small by the time nonlinear effects come into play so that the latter are initially confined to the critical layer.

The nonlinear interaction of a pair of oblique instability waves was first considered by Goldstein & Choi (1989) for Rayleigh waves in a free shear layer. They studied such an interaction in the non-equilibrium critical layer regime, and showed that the nonlinear evolution of the oblique wave amplitude is governed by an integro–differential equation, of the type first derived by Hickernell (1984) in a somewhat different context. In the inviscid case they considered, their results showed that the solution to this equation ends in a singularity at a finite downstream position. The rapid growth of the amplitude as the singularity is approached is now often referred to as 'explosive growth'. Their analysis also showed that the critical-layer interaction produces a relatively large mean-flow distortion in the whole flow field.

The analysis of Goldstein & Choi (1989) was extended to include the effects of viscosity by Wu, Lee & Cowley (1993) who found that the amplitude of the waves either ends in the same singularity as the inviscid case, or undergoes exponential decay after reaching a peak, depending upon the parameter values. They further showed that in the latter case, the nonlinearly induced mean flow still grows algebraically.

Since the critical-layer nonlinearity is generic and not dependent upon the details of the mean flow, essentially the same integro–differential equation describes the amplitude of a pair of oblique waves in any inviscidly unstable flow. For instance, Leib & Lee (1995) considered the case of a two-dimensional supersonic boundary layer, while Wundrow & Goldstein (1994) and Goldstein & Wundrow (1995) considered a weakly three-dimensional subsonic boundary layer. In both these cases, the rapid growth of the amplitude to form a singularity and the development of a relatively large mean-flow distortion are the dominant features of the interaction.

Smith, Brown & Brown (1993) considered similar interactions in the equilibrium critical layer regime relating to the start-up of the wave/vortex interaction. This analysis was extended to the unequal-amplitude case by Brown & Smith (1996).

In an incompressible plane Blasius boundary layer or a plane Poiseuille flow, transition occurs due to the nonlinear development of viscous T-S waves. Hall & Smith (1989) and Smith & Blennerhassett (1992) investigated the nonlinear interaction

of a pair of oblique T-S waves which are close to the lower branch of the neutral curve. One of their important findings is that the interaction between the waves can drive a very large spanwise-dependent mean-flow distortion, and as a result the dominant nonlinear interaction is between the wave and the induced mean flow, while the harmonic does not play an active role. Hall & Smith (1989) refer to such a feature as wave/vortex interaction. Blackaby (1994) and Davis & Smith (1994) further considered this type of T-S wave/vortex interaction in hypersonic and three-dimensional incompressible boundary layers, respectively.

Another approach to analysing instability wave interactions is by direct numerical simulations using the Navier–Stokes equations. For example, simulations of oblique wave interactions in a Blasius boundary layer were performed by Joslin, Streett & Chang (1993). They found that the interactions can induce an enhanced growth provided that initial amplitudes are sufficiently high. Simulations in a low-supersonic-Mach-number flat plate boundary layer have been carried out by, among others, Fasel, Thumm & Bestek (1993) (see references therein). The simulations show that the oblique wave interaction generates a strong spanwise-dependent mean-flow distortion, consistent with the prediction of the asymptotic theory.

On the other hand, Schmid & Henningson (1992*a*, *b*) simulated the transition initiated by a pair of oblique waves in the plane Poiseuille flow in the sub-critical Reynolds number range. They find that both spanwise-dependent and spanwise-independent mean flows undergo significant growth, but they attribute such a growth to a linear mechanism. Also, in their calculations the spanwise-independent mean flow is found to be one order of magnitude larger than the spanwise-dependent mean flow.

In this paper, we study the interaction between a pair of oblique T-S modes in the Blasius boundary layer. However, unlike Hall & Smith (1989) and Smith & Blennerhassett (1992), we now consider the *upper-branch scaling regime*. This is motivated by the fact that in most experiments on boundary-layer transition, significant nonlinear activities do not take place until the upper branch is approached (e.g. Klebanoff, Tidstrom & Sargent 1962; Kachanov & Levchenko 1984; Corke & Mangano 1989). Mathematically, analytical progress in the upper-branch scaling regime becomes more feasible because the linear growth rate is asymptotically smaller than the wavenumber. Furthermore, as pointed out by Goldstein & Durbin (1986), this scaling applies to almost the entire linearly unstable region, including the overlap domain between the upper- and lower-branch regions, i.e. the high-frequency limit of the lower-branch scaling. In contrast, weakly nonlinear analyses based on the lower-branch scaling are valid only in an asymptotically small neighbourhood of the lower-branch. We are aware of the fact that the upper-branch asymptotics do not approximate the linear growth rate accurately enough at moderately high Reynolds numbers† (Reid 1965; Healey 1994). However, the nonlinear growth rates should not be subject to such inaccuracy and the quantitative behaviour of the solution in the nonlinear regime should only be minimally affected by the linear result. This is because the size of the linear growth rate simply shifts the streamwise location at which nonlinearity comes into play, and once entering the nonlinear regime the nonlinear growth rate quickly overtakes the linear one. We expect the nonlinear growth rates to be more accurately predicted than the linear growth rates because the former eventually become larger than the latter and therefore correspond, in

† L. Hultgren (1996, private communication) has found that by renormalizing the asymptotic results, it is possible to achieve significant improvement in the accuracy of the linear asymptotic theory.

effect, to a lower-order term in the asymptotic expansion. The main reason for the inaccuracy of the linear theory is that the growth rates, which correspond to the imaginary part of the wavenumber, are of much higher order than the wavenumber itself. Also, although a finite-Reynolds-number approach, i.e. the Orr–Sommerfeld equation, gives a good approximation to a linear growth rate, it seems impossible, in this framework, to extend weakly nonlinear theory to an unbounded flow such as a boundary layer. This is because there is a fundamental difficulty in accommodating the nonlinearly induced mean flow on a finite-Reynolds-number basis. We believe that a high-Reynolds-number asymptotic approach must be used in order to analyse rigorously the oblique-mode interactions in a boundary layer.

The rest of the paper is organized as follows. In §2, the problem is formulated and the linear solution is presented. The first nonlinear stage is considered in §3, where we show that nonlinearity only affects the wavelength while leaving the modulus of the disturbance to evolve linearly. Since the analysis in these two sections is, for the most part, contained in previous work, details are omitted from the present paper. In §4, we show that the continuing wavelength alteration will eventually have an impact on the modulus, leading the disturbance into the second nonlinear stage where the amplitude function takes a WKBJ form with the phase and the modulus evolving over different streamwise length scales. By a detailed analysis of the nonlinear dynamics within the critical layer and the diffusion layer, we derive the coupled equations governing the development of the phase and the modulus. It is shown that the solution to these equations develops a singularity at a finite distance downstream. In §5, by analysing the scaling change associated with the formation of the singularity, we show that in the vicinity of the singularity, the disturbance enters a third stage where the waves evolve over a faster streamwise scale than in the previous stage and non-equilibrium critical layer effects influence the development. By observing the similarity between the present problem and the related problem on Rayleigh waves considered by Wu *et al.* (1993), it is found that the governing amplitude equation in this stage is the same as that in the Rayleigh problem but without the linear growth term. The appropriate initial condition for this stage is derived by matching with the previous stage and in Appendix B we show that this condition is consistent with the amplitude equation. The amplitude equation is solved numerically, and it is found that the solution develops another finite-distance singularity. The latter is the same as that originally found by Goldstein & Choi (1989) and leads to a strongly nonlinear stage, governed by the unsteady three-dimensional inviscid triple-deck equations. This final stage is highlighted in §6.

It had previously been suggested (Goldstein 1994; Lee 1994) that the continued wavelength shortening caused by the initial nonlinear stage could lead to a stage with a non-equilibrium nonlinear critical layer with the amplitude governed by a limiting form of the equation derived by Wu *et al.* (1993). The present analysis shows that this is indeed the case. In fact, it is shown in Appendix C that all the weakly nonlinear stages through which the oblique T-S waves evolve are governed by limiting forms of the amplitude equation derived by Wu *et al.* (1993) for the nonlinear non-equilibrium viscous critical layer regime. In §7 we discuss the implications of this and draw some general conclusions from the results of our analysis.

2. Formulation and linear solutions

The basic flow is taken to be the incompressible Blasius boundary layer on a flat plate. It is described in terms of Cartesian coordinates (x, y, z) with origin at a point

on the plate a (dimensional) distance L downstream from the leading edge, where x and y are along and normal to the plate respectively, and z is the spanwise direction. The velocity, length, time and pressure are normalized by U_∞, δ^*, δ^*/U_∞ and ρU_∞^2 respectively, where U_∞ is the free-stream velocity, ρ is the fluid density, ν is the kinematic viscosity, and $\delta^* = (\nu L/U_\infty)^{1/2}$ is the boundary-layer thickness at $x = 0$. The local Reynolds number is $R = U_\infty \delta^*/\nu$. The basic-flow profile close to the wall has the asymptotic behaviour

$$U_B \sim \lambda y + \lambda_4 y^4 + \dots \quad \text{as} \quad y \to 0, \tag{2.1}$$

where $\lambda_4 = -\lambda^2/48$. Strictly speaking, λ depends on the slow streamwise variable x/R. But to the order of approximation in the present paper, it can be treated as constant with $\lambda \approx 0.332$.

Let us suppose that a pair of oblique T-S waves with a common dimensional frequency Ω, modulated in the streamwise direction, are superimposed upon this base flow. The upper-branch regime for the Blasius boundary layer corresponds to the scaling†

$$R \sim (\Omega\nu/U_\infty^2)^{-5/6} . \tag{2.2}$$

It is convenient to introduce a small parameter

$$\sigma = R^{-1/10} ,$$

and to define a scaled frequency $\omega = \sigma^{-12}(\Omega\nu/U_\infty^2)$. Linear theory (e.g. Bodonyi & Smith 1981) suggests the introduction of scaled coordinates

$$X = \sigma\alpha x - \sigma^2\omega t , \quad Z = \sigma\beta z , \quad x_1 = \sigma^4 c^{-1} x , \tag{2.3}$$

where X and Z are 'fast' variables describing the oscillation and the spanwise variation of T-S waves respectively, while x_1 is an appropriate 'slow' variable describing the growth of the T-S waves. The parameters α and β are the scaled streamwise and spanwise wavenumbers respectively, and c is the phase speed of the disturbance. We thus have the multiple-scale substitutions:

$$\frac{\partial}{\partial t} \to -\sigma^2\omega\frac{\partial}{\partial X} , \quad \frac{\partial}{\partial x} \to \sigma\alpha\frac{\partial}{\partial X} + \sigma^4 c^{-1}\frac{\partial}{\partial x_1} , \quad \frac{\partial}{\partial z} \to \sigma\beta\frac{\partial}{\partial Z} . \tag{2.4}$$

In addition, the wavenumber α and the phase speed c expand in the form

$$\alpha = \alpha_0 + \sigma\alpha_1 + \sigma^2\alpha_2 + \sigma^3 \ln\sigma\alpha_{3L} , \tag{2.5}$$

$$c = \omega/\alpha = c_0 + \sigma c_1 + \dots , \quad \text{with} \quad c_0 = \omega/\alpha_0 , \quad \text{etc.} \tag{2.6}$$

However, we shall only need to retain leading-order terms in the expansions as higher-order ones do not affect the nonlinear interactions considered in this paper. In terms of the above scaled variables, the disturbance in the main part of the boundary layer, to leading order, takes the form

$$u = \epsilon A(x_1)\bar{u}_1(y)\,\mathrm{e}^{\mathrm{i}X}\cos Z + \text{c.c.} + \dots , \tag{2.7}$$

$$v = -\epsilon\sigma\gamma\,\mathrm{i}\,A(x_1)\bar{v}_1(y)\,\mathrm{e}^{\mathrm{i}X}\cos Z + \text{c.c.} + \dots , \tag{2.8}$$

† After minor modifications to the asymptotic scalings, our analysis is also applicable to boundary layers driven by pressure gradients. For example, for a boundary layer with a favourable pressure gradient, the appropriate scaling is $R \sim (\Omega\nu/U_\infty^2)^{-3/4}$ (e.g. Reid 1965; Smith & Bodonyi 1982). This scaling is also relevant to boundary layers with adverse pressure gradients, but only for disturbances with wavelengths much longer than those of the most unstable modes.

$$w = \epsilon A(x_1)\bar{w}_1(y)\,\mathrm{e}^{\mathrm{i}X}\sin Z + \text{c.c.} + \dots\ , \tag{2.9}$$

$$p = \epsilon\sigma A(x_1)\bar{p}_1(y)\,\mathrm{e}^{\mathrm{i}X}\cos Z + \text{c.c.} + \dots\ , \tag{2.10}$$

where ϵ is a measure of the magnitude of the disturbance, and $A(x_1)$ is the (scaled) amplitude function describing the slow downstream development of the disturbance. For convenience, we have defined

$$\gamma = (\alpha_0^2 + \beta^2)^{1/2}\ .$$

Here and below c.c. represents the complex conjugate.

As pointed out by Bodonyi & Smith (1981), the linear instability problem is described by a multi-layer structure with five asymptotic regions: the potential-flow zone (I), the main layer (II), the Tollmien layer (III), the Stokes layer (IV), and the critical layer (V). These layers have thickness of order σ^{-1}, 1, σ, σ^4 and σ^3 respectively. We obtain the solution in each of the regions by expanding in terms of the small parameter σ. This procedure† can be carried out along the lines of Bodonyi & Smith (1981), and was followed by Wu, Stewart & Cowley (1996) and Wu (1993). Some details can be found in the first paper. Matching between different zones gives the leading-order dispersion relation

$$\lambda c_0 = \gamma\ , \tag{2.11}$$

and the growth rate

$$c_0^{-1}(\cos\theta + \sec\theta)A'/A = -2\mu c_0 Y_c(\Delta\phi) + \lambda^2(2\alpha_0 c_0)^{-1/2} + \mathrm{i}\,\chi\ , \tag{2.12}$$

where

$$\theta = \sin^{-1}\beta/\gamma\ , \quad Y_c = c_0/\lambda\ , \quad \mu = -c_0^2/4\ . \tag{2.13}$$

The first term on the right-hand side of (2.12) is the jump across the critical layer, while the second term is the viscous growth rate produced by the Stokes layer adjacent to the wall. In the linear regime,

$$\Delta\phi = -\pi\ .$$

The parameter χ in (2.12) is a real number. It represents an $O(\sigma^3)$ correction to the wavenumber, and can be conveniently absorbed into the carrier wave $\mathrm{e}^{\mathrm{i}X}$ by adding the term of $\sigma^3(\cos\theta + \sec\theta)^{-1}\chi$ into (2.5).

3. Nonlinear stage I: wavelength 'shortening'

The first nonlinear regime is reached when the nonlinear effect on the modulation of the disturbance is at the same order as the linear effect. This occurs when (cf. Mankbadi *et al.* 1993)

$$\epsilon = \sigma^8\ . \tag{3.1}$$

The analysis of interactions in this regime is essentially contained in Wu (1993) and Mankbadi, Wu & Lee (1993) in their studies of a subharmonic resonant triad. It is shown there that when nonlinear effects are included two extras layers, namely a diffusion layer (VI) sandwiching the critical level and a buffer layer (VII) adjacent to the wall, have to be introduced in order to accommodate the induced spanwise-dependent mean-flow distortion. The disturbance is thus described by a seven-zoned structure. Dominant nonlinear effects arise from the critical layer (V) and the diffusion

† A different but somewhat related approach was used by Mankbadi, Wu & Lee (1993) and Goldstein & Lee (1992).

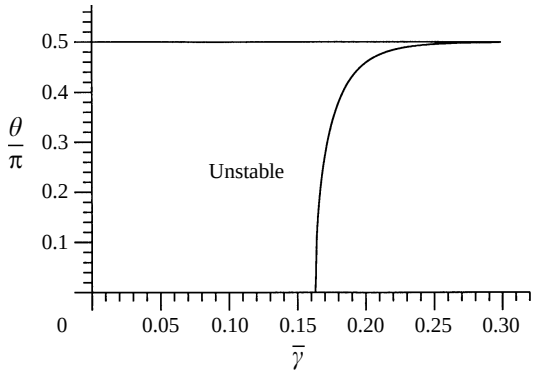

FIGURE 1. The region of the parameters (γ, θ) over which oblique modes are unstable.

layer (VI), while the wall-buffer layer (VII) plays a passive role. The amplitude equation is

$$\frac{\mathrm{d}A}{\mathrm{d}x_1} = \kappa A + \mathrm{i}\,\Upsilon A \int_0^{+\infty} |A(x_1 - \zeta)|^2\,\mathrm{d}\zeta\ , \tag{3.2}$$

where

$$\kappa = c_0(\cos\theta + \sec\theta)^{-1}\left[\lambda^2(2\alpha_0 c_0)^{-1/2} + 2c_0^2\lambda^{-1}\mu\pi\right]\ , \tag{3.3}$$

$$\Upsilon = -\left(\tfrac{2}{3}\right)^{2/3}\Gamma\left(\tfrac{1}{3}\right)\pi\gamma^2 c_0^5\lambda^{1/3}\alpha_0^{1/3}\sin^4\theta\cos 2\theta(\cos\theta + \sec\theta)^{-1}\ . \tag{3.4}$$

These results were obtained by extending the analysis of Wu (1993) and Mankbadi *et al.* (1993) to allow for the fact that θ is no longer restricted to 60° but can vary arbitrarily in the present study. Equation (3.2) is subject to the initial condition

$$A \to A_0\,\mathrm{e}^{\kappa x_1} \quad \text{as} \quad x_1 \to -\infty\ ,$$

in order to ensure that the solution matches to the linear stage upstream.

The linear growth rate κ depends on θ, the obliqueness angle. Since we are only interested in growing modes, we require $\kappa > 0$. It follows from (3.3), (2.11) and (2.13) that θ must satisfy

$$\cos\theta < 2\lambda^{15}/(\pi^2\gamma^{10})\ .$$

The above condition is satisfied for any θ if $\gamma \leqslant \gamma_c \equiv 2^{1/10}\pi^{-1/5}\lambda^{3/2}$. However, if $\gamma > \gamma_c$, then κ is positive only for waves which are sufficiently oblique with

$$\theta > \cos^{-1}(2\pi^{-2}\lambda^{15}\gamma^{-10})\ .$$

In the parameter space (γ, θ), the region in which oblique modes are unstable is indicated in figure 1.

The nonlinear term arises from an interaction between the oblique modes and the induced spanwise-dependent mean flow, characteristic of wave–vortex interactions. However, unlike the lower-branch scaling (cf. Smith & Blennerhassett 1992), the coefficient of the nonlinear term is purely imaginary in the present upper-branch-scaling regime. An important consequence is that only the phase angle of the amplitude function is affected by nonlinearity, while its modulus still evolves exponentially, as in the linear regime. In order to illustrate this more clearly, we write

$$A = |A|\,\mathrm{e}^{\mathrm{i}\,\Theta(x_1)}\ .$$

Then $|A|$ and $\Theta(x_1)$ satisfy

$$\frac{\mathrm{d}|A|}{\mathrm{d}x_1} = \kappa|A| \ , \quad \frac{\mathrm{d}\Theta}{\mathrm{d}x_1} = \Upsilon \int_0^{+\infty} |A(x_1-\zeta)|^2 \,\mathrm{d}\zeta \ .$$

Obviously the modulus $|A|$ and the phase Θ are decoupled, with the phase playing a passive role. The above equations can be easily solved to give

$$|A| = |A_0|\,\mathrm{e}^{\kappa x_1} \ , \quad \Theta = \Theta_0 + \Upsilon|A_0|^2\,\mathrm{e}^{2\kappa x_1}/(2\kappa)^2 \ , \tag{3.5}$$

and hence

$$A = |A_0|\,\mathrm{e}^{\kappa x_1 + \mathrm{i}\,\Theta_0 + \mathrm{i}\,\Upsilon|A_0|^2\,\mathrm{e}^{2\kappa x_1}/(2\kappa)^2} \ , \tag{3.6}$$

where $\Theta_0 = \arg A_0$, and shall be assumed to be zero without losing generality. Note that Θ' can be regarded as the wavelength alteration due to nonlinear effects. The second equation in (3.5) implies that the rate at which the wavelength 'shortens' is exponential.

4. Nonlinear stage II: wavelength-shortening-induced nonlinearity

The rapid modulation of the phase will eventually have an impact on the development of the modulus. This occurs when†

$$x_1 = O(\kappa^{-1}\log\sigma^{-3/8}) \ , \tag{4.1}$$

and we thus introduce the shifted coordinate

$$\hat{x} = x_1 - \kappa^{-1}\log\sigma^{-3/8} \ . \tag{4.2}$$

For $\hat{x} = O(1)$, the magnitude of the disturbance rises to

$$\hat{\epsilon} = \epsilon\sigma^{-3/8} = \sigma^{61/8} \ . \tag{4.3}$$

The disturbance in the main part of the flow still can be expanded as (2.7)–(2.10) except that ϵ is replaced by $\hat{\epsilon}$. The amplitude function in this stage takes the WKBJ form

$$A(\hat{x}) = \hat{A}(\hat{x})\,\mathrm{e}^{\mathrm{i}\,\hat{\Theta}(\hat{x})/\sigma^{3/4}} \ , \tag{4.4}$$

as implied by (3.6). Then we have the multiple-scale substitution

$$\frac{\partial}{\partial x} \to \sigma\alpha\frac{\partial}{\partial X} + \sigma^{13/4}c^{-1}\hat{\Theta}'\frac{\partial}{\partial\hat{\Theta}} + \sigma^4 c^{-1}\frac{\partial}{\partial x_1} \ . \tag{4.5}$$

It turns out that $\hat{\Theta}$ and $\hat{A}$ should expand as

$$\hat{\Theta} = \hat{\Theta}_0 + \sigma^{1/2}\hat{\Theta}_1 \ , \quad \hat{A} = \hat{A}_0 + \sigma^{1/2}\hat{A}_1 + \ldots \ . \tag{4.6}$$

In the present stage, the evolution is described by the leading-order terms $\hat{A}_0$ and $\hat{\Theta}_0$. However, the higher-order corrections, $\hat{A}_1$ and $\hat{\Theta}_1$, will become as important as $\hat{A}_0$ and $\hat{\Theta}_0$ towards the end of this stage, and hence will affect the matching with the following stage, stage III. In order to simplify the algebra, we do not break up $\hat{\Theta}$ and

† Identifying this distinguished distance is part of the solution process. It involves a careful consideration of the wavelength-shortening-induced velocity components (4.18) and (4.19), their subsequent interaction with the leading-order wave components and the mean flow so induced, i.e. (4.34) and (4.35). The scaling is derived by further analysing the related solutions in the diffusion layer, (4.54), (4.62), (4.63) and (4.64), and their impact on the critical-layer dynamics (see the comment below (4.64)).

$\hat{A}$ at the very beginning. Instead, we treat them as a whole and proceed to derive the 'composite' equations which are valid up to $O(\sigma^{1/2})$ corrections. The equations for $\hat{A}_0$ and $\hat{\Theta}_0$, and $\hat{\Theta}_1$ and $\hat{A}_1$ will then be obtained by substituting (4.6) into the resulting 'composite' equations.

The overall flow structure remains the same as in stage I. Outside the critical layer and the diffusion layer, the flow is linear up to the order of our interest. A straightforward expansion in each of the layers and matching show that

$$\mathrm{i}\,\gamma c_0^{-1}(\cos\theta+\sec\theta)\frac{\mathrm{d}\hat{\Theta}}{\mathrm{d}\hat{x}} = c_0(a^+ - a^-)\,, \tag{4.7}$$

$$\gamma c_0^{-1}(\cos\theta+\sec\theta)\frac{\mathrm{d}\hat{A}}{\mathrm{d}\hat{x}} = c_0(c^+ - c^-)\,, \tag{4.8}$$

where the jumps $(a^+ - a^-)$ and $(c^+ - c^-)$ are to be determined by analysing the nonlinear dynamics within the critical layer and the surrounding diffusion layer. They are now considered in turn.

4.1. *Critical-layer dynamics*

The critical layer is still in equilibrium and viscosity dominated as in stage I. The transverse variable in this layer is

$$\eta = (y - y_c)/\sigma^3\,, \tag{4.9}$$

where $y_c = \sigma Y_c$. The expansions for the disturbance components are

$$\begin{aligned} u = {} & \hat{\epsilon}\sigma^{-2}\left\{\bar{U}_1 + \sigma^{1/4}\bar{U}_2 + \ldots\right\}\hat{A}\,\mathrm{e}^{\mathrm{i}\hat{\Theta}/\sigma^{3/4}+\mathrm{i}X}\cos Z + \text{c.c.} \\ & + \hat{\epsilon}^2\sigma^{-7}\left\{\sigma^{-1/2}\tau_M\eta^3 + \sigma^{-1/4}\mu_M\eta^2 + U_M^{(1)} + \sigma^{1/4}U_M^{(2)} + \ldots\right\}\cos 2Z + \ldots\,, \end{aligned} \tag{4.10}$$

$$\begin{aligned} v = {} & \left\{\hat{\epsilon}\sigma^2(1+\sigma a)\bar{V}_1 + \hat{\epsilon}\sigma^4\bar{V}_2 + \hat{\epsilon}^3\sigma^{-17/2}\bar{V}_3 + \hat{\epsilon}^3\sigma^{-33/4}\bar{V}_4 + \ldots\right\}\hat{A}\,\mathrm{e}^{\mathrm{i}\hat{\Theta}/\sigma^{3/4}+\mathrm{i}X}\cos Z + \text{c.c.} \\ & + \hat{\epsilon}^2\sigma^{-3}\left\{\sigma^{-1/2}(6\tau_M/\lambda)\eta + \sigma^{-1/4}(2\mu_M/\lambda) + V_M^{(1)} + \sigma^{1/4}V_M^{(2)} + \ldots\right\}\cos 2Z + \ldots\,, \end{aligned} \tag{4.11}$$

$$\begin{aligned} w = {} & \hat{\epsilon}\sigma^{-2}\left\{\bar{W}_1 + \sigma^{1/4}\bar{W}_2 + \ldots\right\}\hat{A}\,\mathrm{e}^{\mathrm{i}\hat{\Theta}/\sigma^{3/4}+\mathrm{i}X}\sin Z + \text{c.c.} \\ & + \hat{\epsilon}^2\sigma^{-7}\left\{\sigma^{-1/2}(-3\tau_M/\lambda\beta) + W_M^{(1)} + \sigma^{1/4}W_M^{(2)} + \ldots\right\}\sin 2Z + \ldots\,, \end{aligned} \tag{4.12}$$

$$p = \hat{\epsilon}\sigma\gamma\cos\theta\hat{A}\,\mathrm{e}^{\mathrm{i}\hat{\Theta}/\sigma^{3/4}+\mathrm{i}X}\cos Z + \text{c.c.} + \hat{\epsilon}^2\sigma^{-2}P_M^{(1)}\cos 2Z + \ldots\,, \tag{4.13}$$

where a is an $O(1)$ constant (see Goldstein & Lee 1992; Mankbadi *et al.* 1993), whose exact value is of no importance in our study. Here harmonics are not included since they do not contribute nonlinear effects to the order considered in the present stage.

An important point is that in order to match to the solution in the diffusion layer, we have to include mean-flow distortions of $O(\hat{\epsilon}^2\sigma^{-15/2})$ and $O(\hat{\epsilon}^2\sigma^{-29/4})$ in (4.10), i.e. the terms involving τ_M and μ_M. Their exact forms are determined by the asymptotic behaviours of the solutions in the diffusion layer, namely (4.63) and (4.64). Note that both terms are larger than the mean-flow distortions that are directly driven by the Reynolds stresses. As we shall show below, it is these two terms that

eventually contribute the nonlinear effect on the modulus; the corresponding vertical and spanwise components do not play any active role.

The solutions for $\bar{V}_1$ and $\bar{V}_2$ are given by

$$\bar{V}_1 = -\mathrm{i}\,\gamma c_0\ , \quad \bar{V}_2 = -\mathrm{i}\,\gamma\lambda\,\eta\ ,$$

which are trivial continuations of the regular terms in the Tollmien-layer expansion (not presented here). The leading-order streamwise and spanwise velocities, $\bar{U}_1$ and $\bar{W}_1$, satisfy

$$[\mathrm{i}\,\alpha_0\lambda\eta - \partial^2/\partial\eta^2]\bar{U}_1 + \lambda(-\mathrm{i}\,\gamma c_0) = -\mathrm{i}\,\alpha_0\gamma\cos\theta\ , \tag{4.14}$$

$$[\mathrm{i}\,\alpha_0\lambda\eta - \partial^2/\partial\eta^2]\bar{W}_1 = \beta\gamma\cos\theta\ . \tag{4.15}$$

These equations can be solved to obtain

$$\bar{U}_1 = \mathrm{i}\,c_0\tan\theta\sin\theta\,\Pi^{(0)}\ , \quad \bar{W}_1 = c_0\sin\theta\,\Pi^{(0)}\ , \tag{4.16}$$

where we have defined

$$\Pi^{(n)} = \int_0^{+\infty}\xi^n\,\mathrm{e}^{-\mathrm{i}\,\eta\xi-\hat{s}\xi^3}\,\mathrm{d}\xi\ , \qquad \hat{s} = \tfrac{1}{3}(\lambda\alpha_0)^{-1}\ . \tag{4.17}$$

The second fundamental components in (4.10) and (4.12), $\bar{U}_2$ and $\bar{W}_2$, are governed by the following equations:

$$[\mathrm{i}\,\alpha_0\lambda\eta - \partial^2/\partial\eta^2]\bar{U}_2 = c_0\tan\theta\sin\theta\hat{\Theta}'(\hat{x})\Pi^{(0)}\ , \tag{4.18}$$

$$[\mathrm{i}\,\alpha_0\lambda\eta - \partial^2/\partial\eta^2]\bar{W}_2 = -\mathrm{i}\,c_0\sin\theta\hat{\Theta}'(\hat{x})\Pi^{(0)}\ . \tag{4.19}$$

The fact that the right-hand sides of (4.18) and (4.19) are proportional to $\hat{\Theta}'$ indicates that $\bar{U}_2$ and $\bar{W}_2$ are induced by the modulation of the phase $\hat{\Theta}(\hat{x})$. We solve the above equations using Fourier transforms, and obtain

$$\bar{U}_2 = (\alpha_0\lambda)^{-1}c_0\tan\theta\sin\theta\hat{\Theta}'(\hat{x})\,\Pi^{(1)}\ , \quad \bar{W}_2 = -\mathrm{i}(\alpha_0\lambda)^{-1}c_0\sin\theta\hat{\Theta}'(\hat{x})\,\Pi^{(1)}\ . \tag{4.20}$$

The continuity equation, $\mathrm{i}\,\alpha_0\bar{U}_2 + \beta\bar{W}_2 = 0$, is satisfied automatically. It can be shown that as $\eta \to \pm\infty$

$$\bar{U}_1 \to (c_0\tan\theta\sin\theta)\eta^{-1}\ , \quad \bar{W}_1 \to (-\mathrm{i}\,c_0\sin\theta)\eta^{-1}\ ; \tag{4.21}$$

$$\bar{U}_2 \to -(\alpha_0\lambda)^{-1}c_0\tan\theta\sin\theta\hat{\Theta}'\,\eta^{-2}\ , \quad \bar{W}_2 \to \mathrm{i}(\alpha_0\lambda)^{-1}c_0\sin\theta\hat{\Theta}'\,\eta^{-2}\ . \tag{4.22}$$

They match to the solutions in the diffusion layer which in turn match with those in the Tollmien layer.

We now examine quadratic interactions within the critical layer. The mean-flow distortion, $U_M^{(1)}$, $V_M^{(1)}$ and $W_M^{(1)}$, is directly driven by the interaction between the leading-order wave components and satisfy

$$\frac{\partial V_M^{(1)}}{\partial\eta} + 2\beta W_M^{(1)} = 0\ , \tag{4.23}$$

$$-\frac{\partial^2 U_M^{(1)}}{\partial\eta^2} + \lambda V_M^{(1)} = -\tfrac{1}{2}\,\mathrm{i}\,\gamma^2\lambda^{-1}c_0\sin\theta\tan\theta|\hat{A}|^2\Pi^{(1)} + \text{c.c.}, \tag{4.24}$$

$$\frac{\partial^2 W_M^{(1)}}{\partial\eta^2} = \tfrac{1}{2}\gamma^2\lambda^{-1}c_0\sin\theta|\hat{A}|^2\left[\Pi^{(1)} + 2\sin^2\theta|\Pi^{(0)}|^2\right] + \text{c.c.} \tag{4.25}$$

Equations (4.23)–(4.25) can be integrated directly. For example,

$$W_M^{(1)} = \gamma^2\lambda^{-1}c_0\sin\theta|\hat{A}|^2[J_w^{(1)} + 4\sin^2\theta J_w^{(2)}] + C\eta + D\ , \tag{4.26}$$

where

$$J_w^{(1)} = \int_0^\infty \frac{2\sin^2 \frac{1}{2}\eta\xi}{\xi} \, \mathrm{e}^{-\hat{s}\xi^3} \, \mathrm{d}\xi \ , \tag{4.27}$$

$$J_w^{(2)} = \int_0^\infty \int_0^{+\infty} \frac{2\sin^2 \frac{1}{2}\eta\xi}{\xi^2} \, \mathrm{e}^{-\hat{s}[(\xi+\zeta)^3+\zeta^3]} \, \mathrm{d}\xi \, \mathrm{d}\zeta \ , \tag{4.28}$$

and C and D are functions of $\hat{x}$. It is found that C must be identically zero to ensure that the $O(\hat{\epsilon}^2\sigma^{-15/2})$ term in (4.10) is continuous at $\eta = 0$. Solutions for $U_M^{(1)}$ and $V_M^{(1)}$ can be obtained in a similar way. As $\eta \to \pm\infty$,

$$W_M^{(1)} \to \pm F_w\eta + H_w \log|\eta| \ , \tag{4.29}$$

$$V_M^{(1)} \to \mp\beta F_w\eta^2 - 2\beta H_w\eta \log|\eta| \ , \tag{4.30}$$

$$U_M^{(1)} \to \mp\tfrac{1}{12}\lambda\beta F_w\eta^4 - \tfrac{1}{3}\lambda\beta H_w\eta^3 \log|\eta| \ , \tag{4.31}$$

where

$$F_w(\hat{x}) = 2\pi\gamma^2\lambda^{-1}c_0 \sin^3\theta q_0|\hat{A}|^2, \quad H_w(\hat{x}) = \gamma^2\lambda^{-1}c_0 \sin\theta\cos 2\theta|\hat{A}|^2, \tag{4.32}$$

$$q_0 = \int_0^{+\infty} \mathrm{e}^{-2\hat{s}\zeta^3} \, \mathrm{d}\zeta = \tfrac{1}{3}(2\hat{s})^{-1/3}\Gamma\left(\tfrac{1}{3}\right) \ . \tag{4.33}$$

The mean-flow distortion, $U_M^{(2)}$, $V_M^{(2)}$ and $W_M^{(2)}$, is driven by the interaction between the leading-order wave components, $\bar{U}_1$, $\bar{V}_1$ and $\bar{W}_1$, and the phase-modulation-induced wave components $\bar{U}_2$ and $\bar{W}_2$. We find that

$$\frac{\partial V_M^{(2)}}{\partial\eta} + 2\beta W_M^{(2)} = 0 \ , \tag{4.34}$$

$$-\frac{\partial^2 U_M^{(2)}}{\partial\eta^2} + \lambda V_M^{(2)} = \tfrac{1}{2}\gamma^3\alpha_0^{-1}\lambda^{-3} \tan\theta \sin\theta\hat{\Theta}'|\hat{A}|^2\Pi^{(2)} + \text{c.c.}, \tag{4.35}$$

$$\frac{\partial^2 W_M^{(2)}}{\partial\eta^2} = -\tfrac{1}{2}\,\mathrm{i}\,\gamma^3\alpha_0^{-1}\lambda^{-3} \sin\theta\hat{\Theta}'|\hat{A}|^2\left[\Pi^{(2)} + 4\sin^2\theta\Pi^{*(0)}\Pi^{(1)}\right] + \text{c.c.} \tag{4.36}$$

The above equation can be solved to give

$$W_M^{(2)} = 2\gamma^3\lambda^{-2} \sin^3\theta\hat{\Theta}'|\hat{A}|^2 Q_w^{(2)} + \dots \ , \tag{4.37}$$

with

$$Q_w^{(2)} = \int_0^{+\infty} \int_0^{+\infty} \frac{\sin\eta\xi - \eta\xi}{\xi} \, \mathrm{e}^{-\hat{s}[(\xi+\zeta)^3+\zeta^3]} \, \mathrm{d}\xi \, \mathrm{d}\zeta \ ; \tag{4.38}$$

the dots in (4.37) indicate that we have ignored the terms which vanish at the edge of the critical layer (and hence do not affect the diffusion layer dynamics). The solutions for $V_M^{(2)}$ and $U_M^{(2)}$ can be obtained by straightforward substitution and integration, and the details are omitted. As $\eta \to \pm\infty$,

$$W_M^{(2)} \to \pm I_w \ , \quad V_M^{(2)} \to \mp 2\beta I_w\eta \ , \quad U_M^{(2)} \to \mp\tfrac{1}{3}\beta\lambda I_w\eta^3 \ , \tag{4.39}$$

where

$$I_w(\hat{x}) = 2\pi\gamma^3\alpha_0^{-1}\lambda^{-3} \sin^3\theta q_0\hat{\Theta}'(\hat{x})|\hat{A}|^2 \ .$$

Because the mean-flow distortions become unbounded at the edge of the critical layer, a diffusion layer must be introduced to bring in the slow streamwise variation

effect of the induced mean flow (cf. Wu 1993; Mankbadi *et al.* 1993). This will be considered in the next subsection.

The $O(\hat{\epsilon}^3\sigma^{-17/2})$ term in (4.11), $\bar{V}_3$, satisfies

$$\left[\mathrm{i}\,\alpha_0\lambda\eta - \partial^2/\partial\eta^2\right]\bar{V}_{3,\eta\eta} = \alpha_0\gamma^2\lambda^{-1}\tau_M\left[3\eta - 2\,\mathrm{i}\sin^2\theta(\eta^3\Pi^{(0)})_\eta\right], \tag{4.40}$$

where the right-hand side represents the Reynolds stress produced by the interaction between the $O(\hat{\epsilon}^2\sigma^{-15/2})$ mean flow in (4.10) and the leading-order wave components. After solving equation (4.40), we find that

$$\bar{V}_{3,\eta\eta} = -\,\mathrm{i}\,\gamma^2\lambda^{-2}(3 - 4\sin^2\theta)\tau_M + \dots\,, \tag{4.41}$$

where we have only written out the part of the solution that is relevant for the derivation of the amplitude equations.

Next, we solve for $\bar{V}_4$ in (4.11), which will contribute a jump across the critical level Y_c. It is found that the governing equation for $\bar{V}_4$ is

$$\left[\mathrm{i}\,\alpha_0\lambda\eta - \partial^2/\partial\eta^2\right]\bar{V}_{4,\eta\eta} = 2\alpha_0\gamma\mu c_0\hat{A}(\hat{x}) - \gamma^2\lambda^{-2}(3 - 4\sin^2\theta)\tau_M\hat{\Theta}' + R_1 + R_2\,, \tag{4.42}$$

where

$$R_1 = -2\alpha_0\gamma\lambda^{-2}\tan\theta\sin\theta\hat{\Theta}'\tau_M\left(\eta^2\Pi^{(1)}\right)_\eta\,,$$

$$R_2 = \alpha_0\gamma^2\lambda^{-1}\mu_M\left[1 - 2\,\mathrm{i}\sin^2\theta\left(\eta^2\Pi^{(0)}\right)_\eta\right].$$

They are the Reynolds stresses generated by the interaction between the $O(\hat{\epsilon}^2\sigma^{-15/2})$ term in (4.10) and the phase-modulation-induced wave components, and the interaction between the $O(\hat{\epsilon}^2\sigma^{-29/4})$ term in (4.10) and the leading-order wave components, respectively. The first term on the right-hand side of (4.42) reflects the effect of the curvature of the unperturbed basic flow at the critical layer. Solving (4.42) by Fourier transforms, we obtain

$$\begin{aligned} c^+ - c^- &\equiv \hat{A}\left[V_{4,\eta}(+\infty) - V_{4,\eta}(-\infty)\right] \\ &= 2\gamma c_0\lambda^{-1}\mu\pi\hat{A} + q\hat{A}\int_0^{+\infty}\xi^{-1/2}\left[\hat{\Theta}'(\hat{x}) - \hat{\Theta}'(\hat{x}-\xi)\right]|\hat{A}(\hat{x}-\xi)|^2\,\mathrm{d}\xi, \end{aligned} \tag{4.43}$$

where

$$q = -\pi^{3/2}\gamma c_0^4\tan\theta\sin^3\theta\cos 2\theta\, q_0\,. \tag{4.44}$$

4.2. *Diffusion-layer dynamics*

In the diffusion layer, the 'unsteadiness' balances the viscous effect in the equations governing the mean-flow distortions. This fixes the width of this layer to be $O(\sigma^{5/2})$. The local transverse variable is thus

$$\tilde{\eta} = (y - y_c)/\sigma^{5/2}\,. \tag{4.45}$$

Equations (4.9)–(4.12), (4.21), (4.22), (4.29)–(4.31) and (4.39) suggest that the expansion in this layer should be

$$\begin{aligned} u = {} & \hat{\epsilon}\sigma^{-3/2}\left\{(c_0\tan\theta\sin\theta)\left[\tilde{\eta}^{-1} + \sigma^{3/4}(-\alpha_0\lambda)^{-1}\hat{\Theta}'\tilde{\eta}^{-2}\right] + \dots\right\}\hat{A}\,\mathrm{e}^{\mathrm{i}\,\hat{\Theta}/\sigma^{3/4} + \mathrm{i}X}\cos Z + \text{c.c.} \\ & + \hat{\epsilon}^2\sigma^{-9}\left\{\tilde{U}_M^{(1)} + \sigma^{1/2}\tilde{U}_M^{(2)} + \sigma^{3/4}\tilde{U}_M^{(3)} + \dots\right\}\cos 2Z + \dots\,, \end{aligned} \tag{4.46}$$

$$v = \left\{\hat{\epsilon}\sigma^2(1+\sigma a)(-\mathrm{i}\,\gamma c_0) + \hat{\epsilon}\sigma^{7/2}(-\mathrm{i}\,\gamma\lambda)\,\tilde{\eta} + \hat{\epsilon}^3\sigma^{-19/2}\tilde{V}_3 + \ldots\right\}\hat{A}\,\mathrm{e}^{\mathrm{i}\,\hat{\Theta}/\sigma^{3/4}+\mathrm{i}X}\cos Z + \text{c.c.}$$
$$+\hat{\epsilon}^2\sigma^{-4}\left\{\tilde{V}_M^{(1)} + \sigma^{1/2}\tilde{V}_M^{(2)} + \sigma^{3/4}\tilde{V}_M^{(3)}\right\}\cos 2Z + \ldots\,, \tag{4.47}$$

$$w = \hat{\epsilon}\sigma^{-3/2}\left\{(-\mathrm{i}\,c_0\sin\theta)\left[\tilde{\eta}^{-1} + \sigma^{3/4}(-\alpha_0\lambda)^{-1}\hat{\Theta}'\tilde{\eta}^{-2}\right] + \ldots\right\}\hat{A}\,\mathrm{e}^{\mathrm{i}\,\hat{\Theta}/\sigma^{3/4}+\mathrm{i}X}\sin Z + \text{c.c.}$$
$$+\hat{\epsilon}^2\sigma^{-15/2}\left\{\tilde{W}_M^{(1)} + \sigma^{1/2}\tilde{W}_M^{(2)} + \sigma^{3/4}\tilde{W}_M^{(3)} + \ldots\right\}\cos 2Z + \ldots\,. \tag{4.48}$$

The governing equations for the leading-order mean-flow distortions are

$$\frac{\partial\tilde{V}_M^{(1)}}{\partial\tilde{\eta}} + 2\beta\tilde{W}_M^{(1)} = 0\,, \tag{4.49}$$

$$\left(\frac{\partial}{\partial\hat{x}} - \frac{\partial^2}{\partial\tilde{\eta}^2}\right)\tilde{U}_M^{(1)} + \lambda\tilde{V}_M^{(1)} = 0\,, \tag{4.50}$$

$$\left(\frac{\partial}{\partial\hat{x}} - \frac{\partial^2}{\partial\tilde{\eta}^2}\right)\tilde{W}_M^{(1)} = 0\,. \tag{4.51}$$

It follows from matching with the critical-layer solutions that the boundary conditions at $\tilde{\eta} = \pm 0$ are

$$\frac{\partial^4\tilde{U}_M^{(1)}}{\partial\tilde{\eta}^4} = \mp 2\beta\lambda F_w\,, \quad \frac{\partial^2\tilde{V}_M^{(1)}}{\partial\tilde{\eta}^2} = \mp 2\beta F_w\,, \quad \frac{\partial\tilde{W}_M^{(1)}}{\partial\tilde{\eta}} = \pm F_w\,. \tag{4.52}$$

Equations (4.49)–(4.51), subject to (4.52), are solved to give

$$\tilde{V}_{M\tilde{\eta}\tilde{\eta}}^{(1)} = -2\beta(4\pi)^{-1/2}\tilde{\eta}\int_0^{+\infty}\zeta^{-3/2}F_w(\hat{x}-\zeta)\exp(-\tilde{\eta}^2/4\zeta)\,\mathrm{d}\zeta\,, \tag{4.53}$$

$$\tilde{U}_{M\tilde{\eta}\tilde{\eta}}^{(1)} = 2\beta\lambda(4\pi)^{-1/2}\tilde{\eta}\int_0^{+\infty}\zeta^{-1/2}F_w(\hat{x}-\zeta)\exp(-\tilde{\eta}^2/4\zeta)\,\mathrm{d}\zeta\,. \tag{4.54}$$

The mean-flow-distortion components at the next order, $\tilde{U}_M^{(2)}$, $\tilde{V}_M^{(2)}$ and $\tilde{W}_M^{(2)}$, are governed by

$$\frac{\partial\tilde{V}_M^{(2)}}{\partial\tilde{\eta}} + 2\beta\tilde{W}_M^{(2)} = 0\,, \tag{4.55}$$

$$\left(\frac{\partial}{\partial\hat{x}} - \frac{\partial^2}{\partial\tilde{\eta}^2}\right)\tilde{U}_M^{(2)} + \lambda\tilde{V}_M^{(2)} = 0\,, \tag{4.56}$$

$$\left(\frac{\partial}{\partial\hat{x}} - \frac{\partial^2}{\partial\tilde{\eta}^2}\right)\tilde{W}_M^{(2)} = H_w(\hat{x})\tilde{\eta}^{-2}. \tag{4.57}$$

Matching with the logarithmic terms in (4.31) gives the following 'boundary conditions'

$$\tilde{U}_M^{(2)} \to -\tfrac{1}{3}\beta\lambda H_w(\hat{x})\tilde{\eta}^3\log|\tilde{\eta}|\,, \quad \tilde{V}_M^{(2)} \to -2\beta H_w(\hat{x})\tilde{\eta}\log|\tilde{\eta}|\,, \quad \tilde{W}_M^{(2)} \to H_w(\hat{x})\log|\tilde{\eta}|\,.$$

In the subsequent calculations, only $\tilde{U}_M^{(2)}$ will be needed, and it is found to be

$$\tilde{U}_{M\tilde{\eta}\tilde{\eta}}^{(2)} = 2\lambda\beta\int_0^{+\infty}\int_0^{+\infty}\xi H_w(\hat{x}-\xi)\,\mathrm{e}^{-k^2\xi}\,k^2\sin(k\tilde{\eta})\,\mathrm{d}\xi\,\mathrm{d}k\,. \tag{4.58}$$

The mean-flow distortion components, $\tilde{U}_M^{(3)}$, $\tilde{V}_M^{(3)}$ and $\tilde{W}_M^{(3)}$, satisfy the same equations as (4.49)–(4.51), but with different boundary conditions

$$\frac{\partial^3 \tilde{U}_M^{(3)}}{\partial \tilde{\eta}^3} = \mp 2\beta\lambda I_w(\hat{x}) \ , \quad \frac{\partial \tilde{V}_M^{(3)}}{\partial \tilde{\eta}} = \mp 2\beta I_w(\hat{x}) \ , \quad \tilde{W}_M^{(3)} = \pm I_w(\hat{x}) \ . \tag{4.59}$$

We find that

$$\tilde{W}_M^{(3)} = (2\pi)^{-1/2}\tilde{\eta}\int_0^{+\infty} \xi^{-3/2} I_w(\hat{x}-\xi)\, \mathrm{e}^{-\tilde{\eta}^2/4\xi}\, \mathrm{d}\xi \ , \tag{4.60}$$

$$\tilde{V}_M^{(3)} = (4\beta/\pi)\int_0^{+\infty}\int_0^{+\infty} I_w(\hat{x}-\xi)\, \mathrm{e}^{-k^2\xi} \cos(k\tilde{\eta})\, \mathrm{d}\xi\, \mathrm{d}k \ , \tag{4.61}$$

$$\tilde{U}_{M\tilde{\eta}\tilde{\eta}}^{(3)} = (4\beta\lambda/\pi)\int_0^{+\infty}\int_0^{+\infty} \xi I_w(\hat{x}-\xi)\, \mathrm{e}^{-k^2\xi}\, k^2 \cos(k\tilde{\eta})\, \mathrm{d}\xi\, \mathrm{d}k \ . \tag{4.62}$$

While the mean-flow distortion components in the diffusion layer are driven by the nonlinear interaction within the critical layer, they also have a back effect on the dynamics in the latter region. This is shown by observing that as $\tilde{\eta} \to 0$,

$$\tilde{U}_M^{(1)} \to \tau_M(\hat{x})\tilde{\eta}^3 \ , \tag{4.63}$$

$$\tilde{U}_M^{(3)} \to \mu_M(\hat{x})\tilde{\eta}^2 \ , \tag{4.64}$$

where

$$\tau_M = \tfrac{1}{6}\pi^{-1/2}\beta\lambda\int_0^{+\infty} \xi^{-1/2} F_w(\hat{x}-\xi)\, \mathrm{d}\xi \ , \tag{4.65}$$

$$\mu_M = \tfrac{1}{2}\pi^{-1/2}\beta\lambda\int_0^{+\infty} \xi^{-1/2} I_w(\hat{x}-\xi)\, \mathrm{d}\xi \ . \tag{4.66}$$

Therefore, the mean-flow expansions in the critical layer must contain the terms proportional to τ_M and μ_M; see (4.10)–(4.12). The quantities τ_M and μ_M can be interpreted, respectively, as the torsion and curvature of the induced mean flow at the critical level.

Finally, we consider the interaction at the cubic level in the diffusion layer. As in stage I, the mean-flow distortion components, $\tilde{U}_M^{(1)}$ and $\tilde{U}_M^{(2)}$, interact with the leading-order wave to produce a velocity jump. It can be obtained by solving for $\tilde{V}_3$, which satisfies

$$\begin{aligned}(\mathrm{i}\,\alpha_0)\lambda\tilde{\eta}\,\tilde{V}_{3,\tilde{\eta}\tilde{\eta}} = {} & \tfrac{1}{2}\,\mathrm{i}\,\alpha_0(-\mathrm{i}\,\gamma c_0)(\tilde{U}_M^{(1)} + \sigma^{1/2}\tilde{U}_M^{(2)})_{\tilde{\eta}\tilde{\eta}} \\ & - 2\alpha_0^2\Big[(c_0 \tan\theta \sin\theta\tilde{\eta}^{-1})(\tilde{U}_M^{(1)} + \sigma^{1/2}\tilde{U}_M^{(2)})\Big]_{\tilde{\eta}} \ .\end{aligned} \tag{4.67}$$

After substituting (4.54) and (4.58) into (4.67), we find that

$$\begin{aligned}a^+ - a^- \equiv {} & \tilde{V}_{3,\tilde{\eta}}(+\infty) - \tilde{V}_{3,\tilde{\eta}}(-\infty) \\ = {} & (-\mathrm{i}\,\gamma\beta c_0 \cos 2\theta)\left\{\int_0^{+\infty} F_w(\hat{x}-\zeta)\, \mathrm{d}\zeta + \sigma^{1/2}(\pi^{3/2}/4)\int_0^{+\infty} \zeta^{-1/2} H_w(\hat{x}-\zeta)\, \mathrm{d}\zeta\right\},\end{aligned} \tag{4.68}$$

where F_w and H_w are defined by (4.32). This jump contributes the nonlinear term in the modulation equation of the phase $\hat{\Theta}(\hat{x})$, as we shall show below.

4.3. *Evolution equations*

Substituting (4.68) and (4.43) into (4.7) and (4.8) respectively, and using (4.32) and (4.44), we obtain the evolution equations for the phase $\hat{\Theta}(\hat{x})$ and the modulus $\hat{A}$:

$$\hat{\Theta}' = \hat{\Upsilon}_\theta \int_0^{+\infty} |\hat{A}(\hat{x}-\xi)|^2 \,\mathrm{d}\xi + \sigma^{1/2}\hat{\Upsilon}_c \int_0^{+\infty} \xi^{-1/2} |\hat{A}(\hat{x}-\xi)|^2 \,\mathrm{d}\xi \,, \tag{4.69}$$

$$\hat{A}' = \kappa\hat{A} + \hat{\Upsilon}_a \hat{A} \int_0^{+\infty} \xi^{-1/2} \Big[\hat{\Theta}'(\hat{x}) - \hat{\Theta}'(\hat{x}-\xi)\Big] |\hat{A}(\hat{x}-\xi)|^2 \,\mathrm{d}\xi \,, \tag{4.70}$$

where $\hat{\Upsilon}_\theta = \Upsilon$ as defined by (3.4), while

$$\hat{\Upsilon}_c = -\tfrac{1}{4}\pi^{3/2}\gamma^2 c_0^5 \sin^2\theta \cos^2 2\theta (\cos\theta + \sec\theta)^{-1} \,,$$

$$\hat{\Upsilon}_a = -\pi^{3/2} c_0^6 \tan\theta \sin^3\theta \cos 2\theta q_0 (\cos\theta + \sec\theta)^{-1} \,,$$

with q_0 being defined by (4.33). The nonlinear terms in the equations for the phase and the modulus come from the diffusion layer and critical layer, respectively. The coupling between the two equations indicates the interplay between the phase and modulus. An interesting feature of equation (4.70) is that if $\hat{\Theta}(\hat{x})$ were a linear function of $\hat{x}$ (as in the linear stage), i.e. if the wavenumber were a constant, then the nonlinear term would vanish. In this sense, the nonlinear effect can be interpreted as arising from wavelength 'shortening' or dilation.

With the $O(\sigma^{1/2})$ term included, equations (4.69) and (4.70) are 'composite', and $\hat{A}$ and $\hat{\Theta}$ should have the expansion (4.6). As mentioned above, the evolution in the present stage is characterized by $\hat{A}_0$ and $\hat{\Theta}_0$, which are governed by

$$\hat{\Theta}_0' = \hat{\Upsilon}_\theta \int_0^{+\infty} |\hat{A}_0(\hat{x}-\xi)|^2 \,\mathrm{d}\xi \,, \tag{4.71}$$

$$\hat{A}_0' = \kappa\hat{A}_0 + \hat{\Upsilon}_a \hat{A}_0 \int_0^{+\infty} \xi^{-1/2} \Big[\hat{\Theta}_0'(\hat{x}) - \hat{\Theta}_0'(\hat{x}-\xi)\Big] |\hat{A}_0(\hat{x}-\xi)|^2 \,\mathrm{d}\xi \,, \tag{4.72}$$

obtained by substituting (4.6) into (4.69), and (4.70) and collecting the leading-order terms. Let us now consider the qualitative behaviour of $\hat{A}_0$. For $\theta < \pi/4$, $\hat{\Upsilon}_\theta < 0$. By differentiating equation (4.71), we find that $\hat{\Theta}_0'' < 0$, and hence $[\hat{\Theta}_0'(\hat{x}) - \hat{\Theta}_0'(\hat{x}-\xi)] < 0$. Since $\hat{\Upsilon}_a < 0$, it then follows from (4.72) that $\hat{A}_0'/\hat{A}_0 > 0$. A similar argument indicates that $\hat{A}_0'/\hat{A}_0$ is positive for $\theta > \pi/4$ as well. We thus conclude that the modulus $\hat{A}_0$ monotonically increases in stage II for virtually any θ. An exception is $\theta \approx \pi/4$, for which the coefficients of the nonlinear terms vanish, and the nonlinear evolution of such waves has to be considered separately.

The equations (4.71) and (4.72) can be combined to give a single equation governing the modulus

$$\hat{A}_0' = \kappa\hat{A}_0 + \hat{\Upsilon}\hat{A}_0 \int_0^{+\infty}\int_0^{+\infty} \xi^{-1/2} \Big[|\hat{A}_0(\hat{x}-\zeta)|^2 - |\hat{A}_0(\hat{x}-\xi-\zeta)|^2\Big] |\hat{A}_0(\hat{x}-\xi)|^2 \,\mathrm{d}\xi \,\mathrm{d}\zeta \,, \tag{4.73}$$

where

$$\hat{\Upsilon} \equiv \hat{\Upsilon}_\theta \hat{\Upsilon}_a = \tfrac{1}{2}\pi^{5/2} \left(\tfrac{2}{3}\right)^{4/3} \Gamma^2\left(\tfrac{1}{3}\right) \gamma^4 c_0^{10} \alpha_0^{-1/3} \lambda^{-1/3} \sin^8\theta \cos^2 2\theta (\cos\theta + \sec\theta)^{-2} \,. \tag{4.74}$$

Equation (4.73) can also be written in the somewhat simpler form

$$\frac{\mathrm{d}\hat{A}_0}{\mathrm{d}\hat{x}} = \kappa\hat{A}_0 + \hat{\Upsilon}\hat{A}_0 \int_{-\infty}^{\hat{x}} \int_{-\infty}^{\xi} \frac{|\hat{A}_0(\zeta)|^2 |\hat{A}_0(\xi)|^2}{(\hat{x}-\zeta)^{1/2}} \,\mathrm{d}\zeta \,\mathrm{d}\xi, \tag{4.75}$$

which is the form actually used for the numerical computations to be presented below. The overall nonlinearity is quintic. Matching with the previous stage gives the initial condition

$$\hat{A}_0(\hat{x}) \to |A_0|\, \mathrm{e}^{\kappa \hat{x}} , \quad \hat{x} \to -\infty , \tag{4.76}$$

which is obviously compatible with (4.73) since the nonlinear term vanishes as $\hat{x} \to -\infty$. It follows from (4.71) that

$$\hat{\Theta}_0(\hat{x}) \to \hat{\Upsilon}_\theta |A_0|^2\, \mathrm{e}^{2\kappa \hat{x}} / (2\kappa)^2 , \tag{4.77}$$

which clearly matches to the solution in stage I (cf. (3.5)).

A numerical solution to (4.75) with (4.76) was computed and is presented in figure 2(*a*) in terms of appropriately normalized variables. The results show the monotonic increase in the modulus described above with the solution developing a singularity at a finite downstream position, say at $\hat{x}_s$. This singularity has the form

$$\hat{A}_0(\hat{x}) \to \frac{\hat{a}_0}{(\hat{x}_s - \hat{x})^{5/8}} \quad \text{as} \quad \hat{x} \to \hat{x}_s , \tag{4.78}$$

where $\hat{a}_0$ is a constant. Substitution of (4.78) into (4.73) gives

$$\tfrac{5}{8} = 4\hat{\Upsilon} J_0 \hat{a}_0^4 , \tag{4.79}$$

which determines $\hat{a}_0$; here

$$J_0 = \int_0^{+\infty} \xi^{-1/2}[(1+\xi)^{1/4} - 1](1+\xi)^{-3/2}\, \mathrm{d}\xi . \tag{4.80}$$

The local asymptotic form near the singularity is shown as the dot–dashed curve in figure 2(*a*) and it is seen that the singularity develops very quickly once the solution departs from the upstream, wavelength-shortening stage, solution. In figure 2(*b*) the result for the corresponding phase function, obtained from (4.71), is shown. It also develops a singularity whose form can be deduced by substituting (4.78) into (4.71), to show that as $\hat{x} \to \hat{x}_s$,

$$\hat{\Theta}_0 \to \phi_0 + \hat{\theta}_0(\hat{x}_s - \hat{x})^{3/4} , \tag{4.81}$$

where ϕ_0 is a constant, and

$$\hat{\theta}_0 = -16\Gamma_\theta \hat{a}_0^2/3. \tag{4.82}$$

Upon inserting (4.6) into (4.69) and (4.70), and collecting all $O(\sigma^{1/2})$ terms, the evolution equations for $\hat{\Theta}_1$ and $\hat{A}_1$ are obtained. As $\hat{x} \to \hat{x}_s$, their solutions develop a singularity of the form

$$\hat{A}_1(\hat{x}) \to \hat{a}_1(\hat{x}_s - \hat{x})^{-9/8} , \quad \hat{\Theta}_1(\hat{x}) \to \hat{\theta}_1(\hat{x}_s - \hat{x})^{1/4} , \tag{4.83}$$

with $\hat{a}_1$ and $\hat{\theta}_1$ being constants. Their values are determined by

$$-\tfrac{1}{4}\hat{\theta}_1 = \tfrac{8}{3}\hat{\Upsilon}_\theta \hat{a}_0 \hat{a}_1 + \hat{\Upsilon}_c I_0 \hat{a}_0^2 , \tag{4.84}$$

$$\tfrac{9}{8}\hat{a}_1 = -\tfrac{1}{4}\hat{\Upsilon}_a \Lambda_0 \hat{a}_0^3 \hat{\theta}_1 - \tfrac{3}{4}\hat{\Upsilon}_a K_0 \hat{\theta}_0 \hat{a}_0^2 \hat{a}_1 , \tag{4.85}$$

where

$$I_0 = \int_0^{+\infty} \zeta^{-1/2}(1+\zeta)^{-5/4}\, \mathrm{d}\zeta , \tag{4.86}$$

$$\Lambda_0 = \int_0^{+\infty} \zeta^{-1/2}\left[1 - (1+\zeta)^{-3/4}\right](1+\zeta)^{-5/4}\, \mathrm{d}\zeta , \tag{4.87}$$

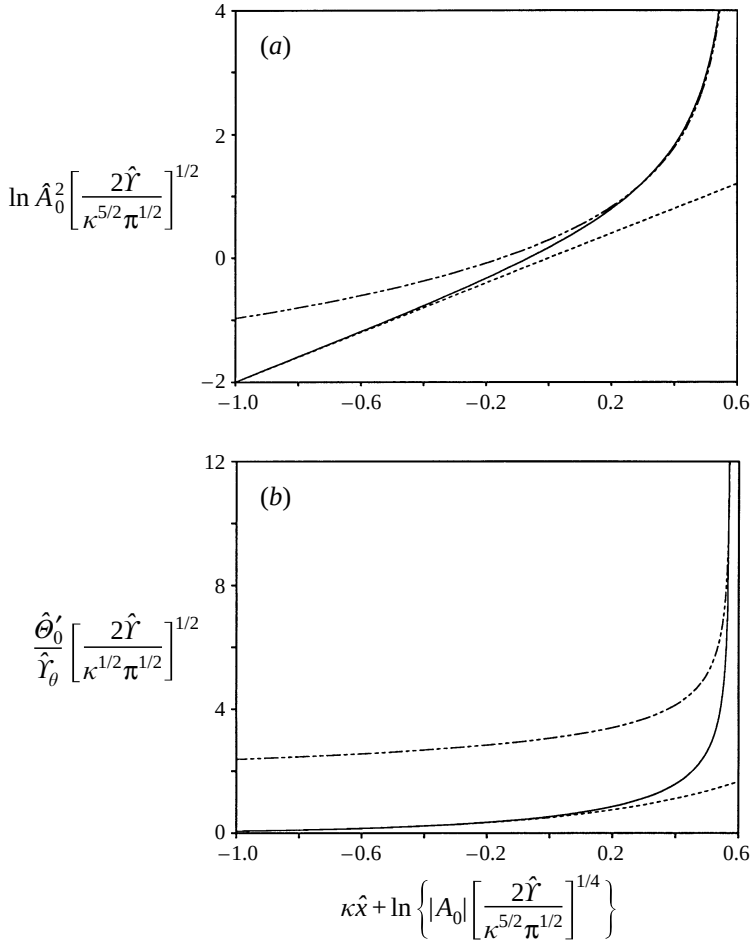

FIGURE 2. (*a*) The normalized modulus, and (*b*) the normalized lowest-order phase function, of the WKBJ solution (soild curve), upstream wavelength-shortening stage solution (dashed), and local asymptotic form near the singularity (dot-dashed) vs. normalized streamwise distance.

$$K_0 = \int_0^{+\infty} \zeta^{-1/2}\left[1-(1+\zeta)^{-1/4}\right](3+\zeta)(1+\zeta)^{-7/4}\,\mathrm{d}\zeta\ . \tag{4.88}$$

It follows from (4.4), (4.6), (4.78), (4.81) and (4.83) that as $\hat{x} \to \hat{x}_s$,

$$A(\hat{x}) \to \left\{\hat{a}_0(\hat{x}_s-\hat{x})^{-5/8} + \sigma^{1/2}\hat{a}_1(\hat{x}_s-\hat{x})^{-9/8}\right\} \times \exp\left\{\mathrm{i}[\hat{\theta}_0(\hat{x}_s-\hat{x})^{3/4} + \sigma^{1/2}\hat{\theta}_1(\hat{x}_s-\hat{x})^{1/4}]/\sigma^{3/4} + \mathrm{i}\,\phi_0/\sigma^{3/4}\right\}\ . \tag{4.89}$$

5. Nonlinear stage III: non-equilibrium critical layer regime

5.1. *Scaling change and amplitude equation*

The singularity structure (4.89) indicates that as $\hat{x} \to \hat{x}_s$,

$$\hat{A}'/\hat{A} \to \tfrac{5}{8}(\hat{x}_s-\hat{x})^{-1}\ .$$

This implies that as a result of the finite-distance singularity, the disturbance will

evolve over a faster spatial scale near $\hat{x}_s$. A new regime is reached when

$$\hat{x}_s - \hat{x} = O(\sigma) \ .$$

In this neighbourhood of $\hat{x}_s$, the critical layer becomes non-equilibrium and viscous in nature, in contrast to stages I and II, where the critical layer is in equilibrium and is purely viscosity dominated. Also, since $\hat{\Theta}' = O(\sigma^{-1/4})$, the first two terms of the wave components in (4.10) and (4.12) are of the same order in magnitude, implying that the phase-modulation-induced velocity becomes as large as the leading-order velocity. The appropriate spatial scale describing the evolution in this stage is

$$\tilde{x} = (\hat{x} - \hat{x}_s)/\sigma \ , \tag{5.1}$$

and the magnitude of the disturbance becomes

$$\tilde{\epsilon} = \hat{\epsilon}\sigma^{-5/8} = \sigma^7 \ . \tag{5.2}$$

The solution in the main part of the boundary layer again takes the form (2.7)–(2.10) provided that ϵ is replaced by $\tilde{\epsilon}$, and $A(x_1)$ by

$$A = \tilde{A}(\tilde{x})\, \mathrm{e}^{\mathrm{i}\,\phi_0/\sigma^{3/4}} \ , \tag{5.3}$$

where $\tilde{A}(\tilde{x})$ is the appropriate complex amplitude function in stage III. The flow outside the critical layer is still linear and inviscid to the order of our interest here, and the solution can be sought by a straightforward expansion. Matching the solutions in different regions gives (see Wu 1995)

$$\mathrm{i}\, c_0^{-1}(\cos\theta + \sec\theta)\frac{\mathrm{d}\tilde{A}}{\mathrm{d}\tilde{x}} = \gamma^2 c_0 (a^+ - a^-) \ , \tag{5.4}$$

where the jump $(a^+ - a^-)$ is to be determined by nonlinear interactions in the critical layer.

To illustrate the major feature of this stage, and also to facilitate the matching with the next stage, we write the first few terms in the expansion within the critical layer:

$$u = \tilde{\epsilon}\sigma^{-2}\left\{(1+\sigma a)\tilde{U}_1 + \sigma^2\tilde{U}_2 + \ldots\right\} \mathrm{e}^{\mathrm{i}\,\phi_0/\sigma^{3/4}+\mathrm{i}X}\cos Z + \text{c.c.} + \ldots \ , \tag{5.5}$$

$$v = \tilde{\epsilon}\sigma^{2}\left\{(1+\sigma a)(-\mathrm{i}\,\gamma c_0)\tilde{A} + \sigma^2(-\mathrm{i}\,\gamma\lambda\tilde{A})\,\eta + \ldots\right\} \mathrm{e}^{\mathrm{i}\,\phi_0/\sigma^{3/4}+\mathrm{i}X}\cos Z + \text{c.c.} + \ldots \ , \tag{5.6}$$

$$w = \tilde{\epsilon}\sigma^{-2}\left\{\tilde{W}_1 + \ldots\right\} \mathrm{e}^{\mathrm{i}\,\phi_0/\sigma^{3/4}+\mathrm{i}X}\sin Z + \text{c.c.} + \ldots \ , \tag{5.7}$$

$$p = \tilde{\epsilon}\sigma\gamma\cos\theta\tilde{A}\, \mathrm{e}^{\mathrm{i}\,\phi_0/\sigma^{3/4}+\mathrm{i}X}\cos Z + \text{c.c.} + \ldots \ , \tag{5.8}$$

where $\tilde{U}_2 = \lambda\sec\theta\tilde{A}$, which is the trivial continuation of the solution in the Tollmien layer. The leading-order streamwise and spanwise velocities, $\tilde{U}_1$ and $\tilde{W}_1$, are governed by equations

$$[\partial/\partial\tilde{x} + \mathrm{i}\,\alpha_0\lambda\eta - \partial^2/\partial\eta^2]\tilde{U}_1 + \lambda(-\mathrm{i}\,\gamma c_0) = -\mathrm{i}\,\alpha_0\gamma\cos\theta \ ,$$

$$[\partial/\partial\tilde{x} + \mathrm{i}\,\alpha_0\lambda\eta - \partial^2/\partial\eta^2]\tilde{W}_1 = \beta\gamma\cos\theta \ .$$

Note that the non-equilibrium effect, represented by $\partial/\partial\tilde{x}$, now appears at leading order. The above equations have the solutions (cf. Wu *et al.* 1993)

$$\tilde{U}_1 = \mathrm{i}\,\gamma^2\sin^2\theta\tilde{\Pi} \ , \quad \tilde{W}_1 = \gamma^2\sin\theta\cos\theta\tilde{\Pi} \ , \tag{5.9}$$

with

$$\tilde{I}\tilde{I} = \int_0^{+\infty} \tilde{A}(\tilde{x}-\xi)\,\mathrm{e}^{-\mathrm{i}\,\alpha_0\lambda\eta\xi - s\xi^3}\,\mathrm{d}\xi\ , \quad s = \tfrac{1}{3}\alpha_0^2\lambda^2\ . \tag{5.10}$$

The nonlinear interactions within the critical layer are the same as in Wu *et al.* (1993) so that the jump across the critical layer, $(a^+ - a^-)$, can be borrowed from there without performing a detailed analysis. After substituting this jump into (5.4), we obtain the amplitude equation

$$\frac{\mathrm{d}\tilde{A}}{\mathrm{d}\tilde{x}} = \mathrm{i}\,\tilde{\Upsilon}\int_0^{+\infty}\int_0^{+\infty} K(\xi,\eta)\tilde{A}(\tilde{x}-\xi)\tilde{A}(\tilde{x}-\xi-\eta)\tilde{A}^*(\tilde{x}-2\xi-\eta)\,\mathrm{d}\xi\,\mathrm{d}\eta\ , \tag{5.11}$$

where

$$\tilde{\Upsilon} = -\pi\gamma^2\alpha_0^3\lambda^3 c_0^5\sin^2\theta(\cos\theta+\sec\theta)^{-1}\ . \tag{5.12}$$

The kernel $K(\xi,\eta)$ is given by (3.85) of Wu *et al.* (1993), with the parameter s given by (5.10). (This kernel is reproduced in Appendix A for completeness.) Similar deductions for nonlinear terms, and associated coefficients, have been made in Wu *et al.* (1996) and Wu (1995), where the critical layers change their character as a result of a focusing singularity and super-exponential growth (induced by subharmonic resonance, see Goldstein 1994), respectively. The term representing the linear growth rate does not enter the amplitude equation (5.11) since the disturbance now evolves over a much shorter streamwise scale.

We note that in the present stage III, the harmonic proportional to $\mathrm{e}^{2\,\mathrm{i}X}$ as well as the spanwise-independent mean flow also make a contribution to the leading-order nonlinear term (see Goldstein & Choi 1989; Wu *et al.* 1993), unlike the two previous stages where the nonlinear effects are solely associated with the induced spanwise-dependent mean flow.

The appropriate initial condition for (5.11) is determined by the requirement that the solution in the present stage match to that in stage II. After rewriting (4.89) in terms of $\tilde{x}$, we have

$$\tilde{A}(\tilde{x}) \to \left\{\hat{a}_0(-\tilde{x})^{-5/8} + \hat{a}_1(-\tilde{x})^{-9/8}\right\}\exp\mathrm{i}\left\{\hat{\theta}_0(-\tilde{x})^{3/4} + \hat{\theta}_1(-\tilde{x})^{1/4}\right\} \tag{5.13}$$

as $\tilde{x}\to-\infty$. In Appendix B, we show that the above condition is compatible with the amplitude equation (5.11) in the sense that both sides of (5.11) have the same asymptotic behaviour when $\tilde{x}\to-\infty$. Hence the solutions in stages II and III indeed match in the asymptotic sense.

A comparison of (5.9) with (4.16) reveals a crucial difference between stages II and III: in stage III, the normal distribution of the leading-order streamwise (and spanwise) velocity(s) undergoes deformation as the amplitude evolves, while in stage II, the normal distribution is solely determined by linear dynamics and does not change its 'shape' during the evolution. Such a deformation of the shape is a direct result of the interplay between nonlinear and non-equilibrium effects. This is one of the important ways that the non-equilibrium critical-layer approach, though weakly nonlinear, differs both from the classical weakly nonlinear theory (cf. Stuart 1960), and from the weakly nonlinear asymptotic theory based on the lower-branch scaling (cf. Hall & Smith 1989; Smith & Blennerhassett 1992).

5.2. *Study of the amplitude equation*

Since the amplitude equation (5.11) does not have a linear term and is subject to an upstream condition different from that in Wu *et al.* (1993), the behaviour of its

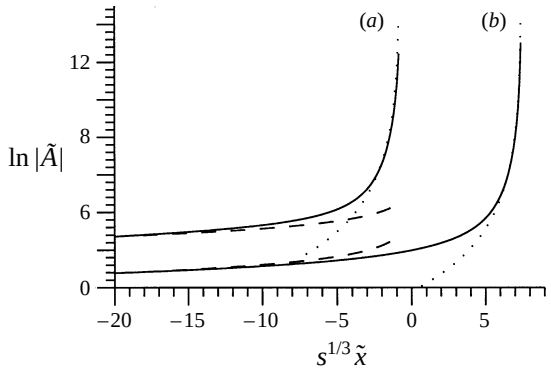

FIGURE 3. Ln|Ã| *vs.* $s^{1/3}\tilde{x}$ for $\gamma = 0.1$: (*a*) $\theta = \pi/8$, (*b*) $\theta = 3\pi/8$. The dashed lines represent the upstream behaviour (5.13), and the dotted lines the local singular solution (5.14).

solution is not immediately clear. In order to resolve this ambiguity, equation (5.11) is solved numerically using an Adam–Moulton finite-difference scheme. In order to march the solution downstream, we begin in the region $\tilde{x} \leqslant -T_0$, $T_0 \gg 1$, where $\tilde{A}$ can be approximated by its asymptote, i.e. by the right-hand side of (5.13). The algebraic decay of $\tilde{A}$ as $\tilde{x} \to -\infty$ in this problem results in a much slower convergence of the double integral in (5.13) (cf. Wu *et al.* 1993). Consequently, attempts to approximate the integral over $D = [0, \infty) \times [0, \infty)$ by integrating over a sufficiently large but finite domain, say $D_0 = [0, X_0] \times [0, Y_0]$, so that the tail over $(D - D_0)$ can be simply ignored, requires extremely large values of (in particular) Y_0. We were unable to obtain reliable results in an acceptable amount of time with this approach. To resolve this difficulty, the tail over $[0, \infty) \times [Y_0, \infty)$ was approximated by its asymptote, while the tail over $[X_0, \infty) \times [0, Y_0]$, which was found to be considerably smaller, was neglected. This allows the required size of Y_0 to be reduced considerably. In fact, we find that it is sufficient to take $X_0 = Y_0 = \tilde{x} + T_0$ with T_0 typically of order 20; halving this size has no appreciable effect on the solution. The smooth matching with the upstream asymptotic behaviour also indicates the reliability of our numerical solution.

Numerical solutions suggest that the amplitude $\tilde{A}(\tilde{x})$ terminates at a singularity at a finite distance, say $\tilde{x}_s$. The singularity takes the form

$$\tilde{A}(\tilde{x}) \to \frac{\tilde{a}_0}{(\tilde{x}_s - \tilde{x})^{3+i\psi}} \qquad \text{as} \qquad \tilde{x} \to \tilde{x}_s \,, \tag{5.14}$$

where $\tilde{a}_0$ and ψ are complex and real numbers respectively. The structure is the same as that proposed by Goldstein & Choi (1989) and Wu *et al.* (1993) for a related amplitude equation. This is not surprising since in the vicinity of the singularity the dominant balance is the same in all the cases.

The amplitude equation (5.11) and the 'initial' condition (5.13) involve only two parameters, γ and θ, which must lie in the unstable region in figure 1. In our calculations, we choose $\gamma = 0.1$, but the results are representative for other values of γ. In figure 3, we show the streamwise development of the modulus of the amplitude $\tilde{A}(\tilde{x})$ for two obliqueness angles: $\theta = \pi/8$ and $\theta = 3\pi/8$. As the figure indicates, starting from the upstream condition (5.13), the disturbance gradually evolves into the new stage as the non-equilibrium effect becomes increasingly significant. For $\theta = \pi/8$, the non-equilibrium effect enhances the amplification, and eventually leads to the formation of a singularity of the form (5.14) at $\tilde{x}_s$. It is found that $\tilde{x}_s < 0$, which indicates that the present singularity is formed prior to the one in the previous

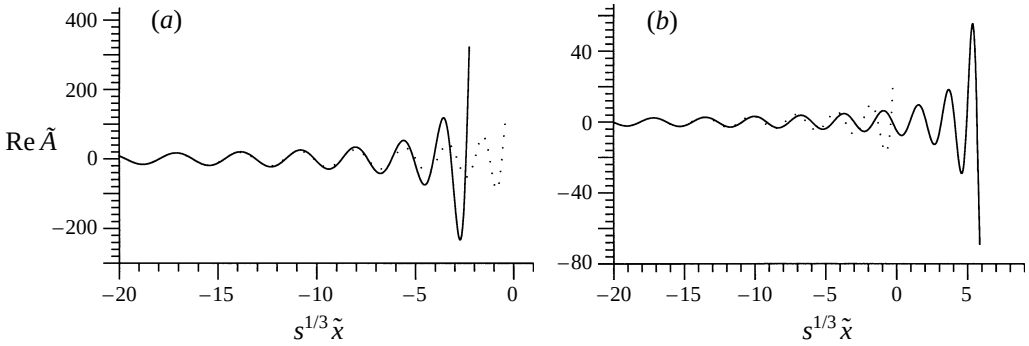

FIGURE 4. Re $\tilde{A}$ *vs.* $s^{1/3}\tilde{x}$ for $\theta = \pi/8$ (*a*) and $\theta = 3\pi/8$ (*b*). The dotted lines represent the upstream behaviour (5.13). Note that the non-equilibrium effect eliminates the singularity of stage II in case (*b*) but not in case (*a*).

stage. For $\theta = 3\pi/8$, the immediate effect of the non-equilibrium critical layer is stabilizing in the sense that it initially inhibits the growth of the disturbance. As a result, the singularity (4.83) in the previous stage is eliminated. However, the ultimate action of the non-equilibrium effect again is to accelerate the amplification, causing a singularity of more severe nature than (4.83). To show the interplay between the wavelength alteration and the nonlinear effect, we plot the development of the real part of the amplitude function in figure 4(*a*,*b*). Clearly, as the disturbance evolves downstream, the wavelength is continually adjusted by nonlinear effects. The change of wavelength in turn affects the modulus. As the singularity is approached, the wavelength will be altered by an $O(1)$ amount.

As indicated above, the non-equilibrium critical layer effects deform the normal distribution of the leading-order streamwise and spanwise velocities. This is shown in figure 5. For $\theta = \pi/8$, the deformation starts with a shifting of the position of the maximum velocity away from the wall, while for $\theta = 3\pi/8$, the position of the maximum descends towards the wall. In both cases, the velocity distribution evolves into a much flatter pattern in the later stage, indicating that the disturbance is no longer concentrated in a thin layer. Such a thickening of the critical layer and the singularity structure (5.14) suggest the introduction of the similarity variable

$$\hat{\eta} = (\tilde{x}_s - \tilde{x})\eta \tag{5.15}$$

to describe the deformation of $\tilde{U}_1$ and $\tilde{W}_1$. Inserting (5.15) and (5.14) into (5.10), and then taking the limit $(\tilde{x} - \tilde{x}_s) \to 0$, we find

$$\tilde{\Pi} \to (\tilde{x}_s - \tilde{x})^{-(2+\mathrm{i}\psi)} \int_0^{+\infty} (1+\xi)^{-(3+\mathrm{i}\psi)}\, \mathrm{e}^{-\mathrm{i}\alpha_0\lambda\hat{\eta}\xi}\, \mathrm{d}\xi\ . \tag{5.16}$$

In figure 6, we plot the distributions of $|\tilde{U}_1|$ at different streamwise stations against $\hat{\eta}$. The shape of $\tilde{U}_1$ appears to approach the final similarity form (5.16) as $\tilde{x} \to \tilde{x}_s$, confirming the asymptotic result.

Our theoretical prediction of disturbance deformation is in broad agreement with the numerical finding of Chang & Malik (1994) for pairs of oblique first modes in a low-Mach-number supersonic boundary layer. This agreement is not too surprising because the same mechanism, namely the interplay between non-equilibrium and nonlinearity, is operative in both flows. In the Chang & Malik simulations, the initial disturbances are T-S waves, but they change their character and become Rayleigh

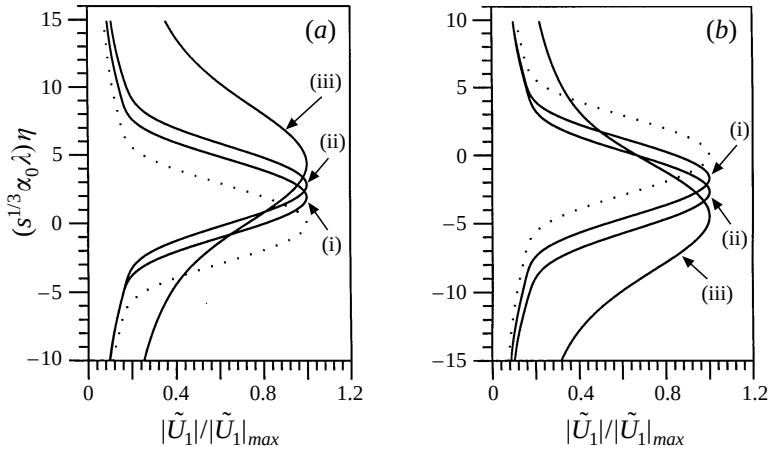

FIGURE 5. The shape of the modulus of streamwise velocity, $|\tilde{U}_1|$, at different downstream locations. (*a*) $\theta = \pi/8$: (i) $s^{1/3}\tilde{x} = -15$, (ii) -5, (iii) -1.55. (*b*) $\theta = 3\pi/8$: (i) $s^{1/3}\tilde{x} = -15$, (ii) 2, (iii) 6.45. The dotted line represents the distribution in the linear regime. The deformation of the shape is characterized by initial drifting and subsequent expanding of the region where the disturbance concentrates.

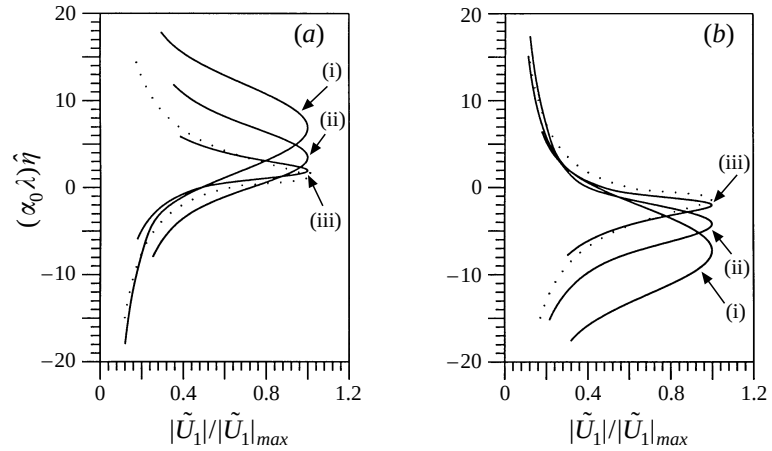

FIGURE 6. Distribution of $|\tilde{U}_1|$ in terms of the similarity variable $\hat{\eta}$. (*a*) $\theta = \pi/8$: (i) $s^{1/3}\tilde{x} = -2.55$, (ii) -1.55, (iii) -1.05. (*b*) $\theta = 3\pi/8$: (i) $s^{1/3}\tilde{x} = 5.75$, (ii) 6.75, (iii) 7.25. The dotted lines correspond to the asymptotic form (5.16).

waves as they approach the upper branch, which is on Rayleigh scaling. The non-equilibrium critical-layer regime can therefore be reached, with the streamwise velocity being exactly the same as (5.9). The amplitude equation (5.11) still applies since compressible effects do not contribute to the dominant nonlinear effect (see Leib & Lee 1995). We believe this similarity is the basis for the agreement.

In a supersonic boundary layer, transition is observed to take place near the critical layer well before the transition reaches the wall. The region of transitional flow expands transversely to form a 'turbulent wedge', which finally spreads to the whole boundary layer (Fischer & Weinstein 1972). This phenomenon may be explained by our theoretical results which show that the disturbance has its largest magnitude in

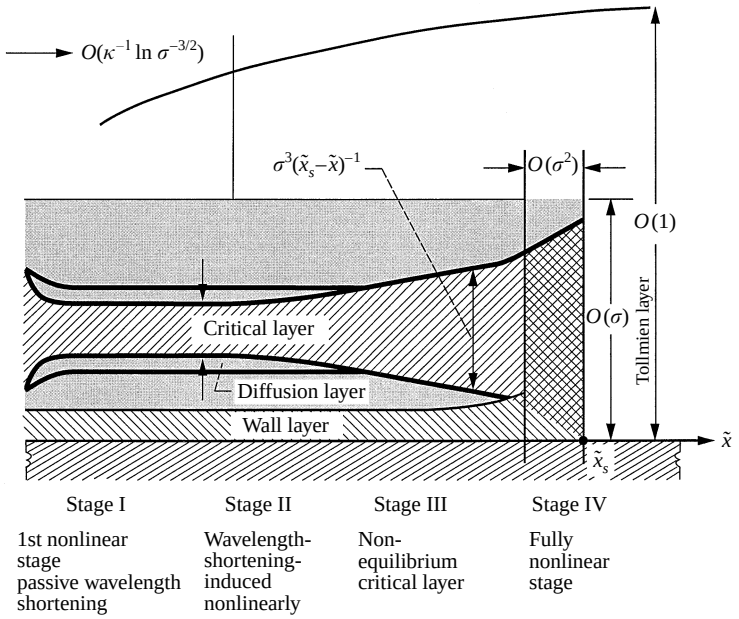

FIGURE 7. Merging of the critical layer with the Tollmien layer.

the critical layer and that the critical layer thickens downstream (see also Pruett & Zang 1992; Pruett & Chang 1995).

6. Nonlinear stage IV: unsteady inviscid triple-deck stage

As $\tilde{x} \to \tilde{x}_s$, the critical layer thickens with its width increasing like $(\tilde{x}_s - \tilde{x})^{-1}$ (see (5.15)), and eventually merges with the Tollmien layer when

$$\tilde{x}_s - \tilde{x} = O(\sigma^2)\ . \tag{6.1}$$

This is shown schematically in figure 7, which also illustrates the flow structures in previous stages. On the other hand, (5.9), (5.10) and (5.16) show that $\tilde{U}_1$ behaves like $(\tilde{x}_s - \tilde{x})^{-(2+\mathrm{i}\psi)}$, while $\tilde{U}_2$, which is proportional to $\tilde{A}$, grows like $(\tilde{x}_s - \tilde{x})^{-(3+\mathrm{i}\psi)}$. Therefore the first two terms in (5.6) become of the same order when (6.1) holds. These suggest that the disturbance enters a new stage in the neighbourhood of $\tilde{x}_s$ specified by (6.1). The unscaled growth rate, $\sigma^3(\tilde{A}'/\tilde{A})$, now increases to $O(\sigma)$, which is of the same order as the wavenumber. The appropriate streamwise variable should be

$$\bar{x} = c\,(\tilde{x} - \tilde{x}_s)/\sigma^2\ . \tag{6.2}$$

All the harmonics have the same order of magnitude as that of the fundamental and the disturbance is no longer sinusoidal in t or Z. The solution will therefore have a more general (but still periodic) dependence on the time and spanwise variables

$$\bar{t} = \sigma^2 t\ , \quad \bar{z} = \sigma z\ .$$

Since the critical layer is no longer distinct, the flow now consists of four layers: the potential layer, the main layer, the Tollmien layer and a viscous wall sublayer (see below). As pointed out by Goldstein (1994), the development of the disturbance is governed by the nonlinear three-dimensional unsteady triple-deck equations. These

equations were derived earlier by Zhuk & Ryzhov (1989) in a more general setting, and the present problem can regarded as a special case of theirs with $\Delta = Re^{-1/20}$.

The transverse variable describing the Tollmien layer is

$$Y = y/\sigma \ .$$

Equations (5.6)–(5.8) together with (5.9), (5.10), (5.16) and (6.2) suggest that the solution in this layer should be expanded as (cf. Zhuk & Ryzhov 1989)

$$(u, v, w, p) = (\sigma U, \sigma^3 V, \sigma W, \sigma^2 P) + \dots \ . \tag{6.3}$$

After substituting the above expansion into the Navier–Stokes equations and retaining leading-order terms, it is found that U, V, W and P satisfy

$$\frac{\partial U}{\partial \bar{x}} + \frac{\partial V}{\partial Y} + \frac{\partial W}{\partial \bar{z}} = 0 \ , \tag{6.4}$$

$$\left.\begin{aligned} \frac{\partial U}{\partial \bar{t}} + U\frac{\partial U}{\partial \bar{x}} + V\frac{\partial U}{\partial Y} + W\frac{\partial U}{\partial \bar{z}} &= -\frac{\partial P}{\partial \bar{x}} \ , \\ \frac{\partial W}{\partial \bar{t}} + U\frac{\partial W}{\partial \bar{x}} + V\frac{\partial W}{\partial Y} + W\frac{\partial W}{\partial \bar{z}} &= -\frac{\partial P}{\partial \bar{z}} \ . \end{aligned}\right\} \tag{6.5}$$

As in standard triple-deck theory (e.g. Smith & Stewart 1987), the pressure P depends only on $\bar{x}$, $\bar{t}$ and $\bar{z}$ (but not on Y), and is related to the displacement $D(\bar{x}, \bar{t}, \bar{z})$ via

$$P = -\frac{1}{2\pi}\int_{-\infty}^{\infty}\int_{-\infty}^{\infty} \frac{\partial^2 D/\partial \xi^2}{[(\bar{x}-\xi)^2 + (\bar{z}-\eta)^2]^{1/2}}\, \mathrm{d}\xi\, \mathrm{d}\eta \ , \tag{6.6}$$

which can be derived by matching the solutions in the potential and the main layers, where the flow is still linear. The boundary condition as $Y \to +\infty$ is given by matching U and W with their counterparts in the main layer, and this leads to (for details see Zhuk & Ryzhov 1989)

$$\left.\begin{aligned} U &\to \lambda Y + D(\bar{x}, \bar{t}, \bar{z}) + \left\{\int_0^{+\infty} \xi P_{\bar{z}\bar{z}}(\bar{x}-\xi, \bar{t}, \bar{z})\, \mathrm{d}\xi\right\} Y^{-1} \ , \\ W &\to \left\{\int_0^{+\infty} P_{\bar{z}}(\bar{x}-\xi, \bar{t}, \bar{z})\, \mathrm{d}\xi\right\} Y^{-1} \ . \end{aligned}\right\} \tag{6.7}$$

The normal velocity vanishes on the wall; so $V = 0$ when $Y = 0$. While Zhuk & Ryzhov (1989) derived the system (6.4)–(6.7), they did not give the appropriate 'initial condition' (in terms of $\bar{x}$) that must be imposed in order to ensure that the system actually describes the later stage of a gradual transition initiated by linear T-S waves in the upstream flow. For the present problem, stage IV follows the merging of the critical layer with the Tollmien layer (see figure 7). The solution should therefore match with the asymptotic behaviour of the critical-layer solution in stage III. After using (5.6)–(5.8), (5.9), (5.10), (5.14)–(5.16) and (6.2), this matching leads to the following 'initial condition':

$$\begin{bmatrix} U-\lambda Y \\ V \\ W \\ P \end{bmatrix} \to \begin{bmatrix} \left(-\mathrm{i}\,\lambda\gamma \sin^2\theta\, \bar{x} G(\bar{x}, Y) + \lambda \sec\theta\right)\cos\beta\bar{z} \\ (-\mathrm{i}\,\gamma\lambda) Y \cos\beta\bar{z} \\ -\lambda\gamma \sin\theta\cos\theta\, \bar{x} G(\bar{x}, Y)\sin\beta\bar{z} \\ \gamma\cos\theta\cos\beta\bar{z} \end{bmatrix} \tilde{a}_0(-\bar{x}/c_0)^{-(3+\mathrm{i}\psi)}\, \mathrm{e}^{\mathrm{i}\phi + \mathrm{i}\alpha(\bar{x}-c\bar{t})} \ ,$$

$$+ \text{c.c.} \quad \text{as} \quad \bar{x} \to -\infty \ , \tag{6.8}$$

where

$$G(\bar{x}, Y) = \int_0^{+\infty} (1+\xi)^{-(3+\mathrm{i}\psi)}\, \mathrm{e}^{\mathrm{i}\,\alpha_0\lambda\bar{x}(Y-Y_c)\xi}\, \mathrm{d}\xi\ , \tag{6.9}$$

which is obtained by rewriting (5.16) in terms of $\bar{x}$ and Y, while

$$\phi = c_0(\hat{x}_s + \kappa^{-1}\log\sigma^{-3/8} + \sigma\tilde{x}_s)/\sigma^3 + \phi_0/\sigma^{3/4}\ .$$

The solution to (6.4)–(6.6) ultimately matches to the initial linear stage, through the intermediate weakly nonlinear stages (i.e. stages I, II and III).

The relevant solution to the triple-deck equations (6.4)–(6.6) satisfies the periodicity condition

$$[U(\bar{t}+T), V(\bar{t}+T), W(\bar{t}+T), P(\bar{t}+T)] = [U(\bar{t}), V(\bar{t}), W(\bar{t}), P(\bar{t})]\ , \tag{6.10}$$

where the period $T = 2\pi/\omega$ since the initial condition is time harmonic. The nonlinear three-dimensional (inviscid) triple-deck system (6.4)–(6.6), subject to (6.7)–(6.10), has not yet been attacked numerically, although some speculations have been made about the possible behaviour of its solution (see §7).

In order to satisfy the no-slip condition on the wall, a wall sublayer with a width of $O(\sigma^4)$ has to be introduced. The transverse variable is $\tilde{Y} = y/\sigma^4$ and the expansion takes the form

$$(u, v, w) = (\sigma\tilde{U}, \sigma^6\tilde{V}, \sigma\tilde{W}) + \dots\ . \tag{6.11}$$

The flow in this layer is driven by the pressure P, which can be prescribed after solving (6.4)–(6.6). It can be shown that $\tilde{U}$, $\tilde{V}$ and $\tilde{W}$ are governed by the classical (non-interactive) unsteady three-dimensional boundary layer equations. Note that, unlike previous stages, the wall sublayer is now fully nonlinear (and for this reason we do not refer to it as a Stokes layer in this section). It is known that the solution to the unsteady classical boundary layer equations usually develops a singularity in the form of a thickening of the displacement (see e.g. Cowley, Van Dommelen & Lam 1991 and references therein). As pointed out by Smith & Burggraf (1985) (see also discussion in Kachanov, Ryzhov & Smith 1993), this may be related, in the present context, to the vorticity eruption from the wall, which was observed to occur in conjunction with spikes (Klebanoff *et al.* 1962).

7. Conclusion and discussion

In this paper, we have followed the nonlinear evolution of a pair of initially linear oblique T-S waves, and presented a self-consistent asymptotic description for the nonlinear stages through which the disturbance evolves. We show that in the initial stage nonlinearity simply alters the wavelength, without affecting the growth of the magnitude of the disturbance. However, once the alteration in the wavelength becomes sufficiently rapid, a back reaction on the disturbance magnitude is produced, leading to the second stage, where the equations governing the development of the wavelength and the disturbance magnitude are coupled (i.e. there is an interplay between the two). The solution develops a singularity at a finite distance downstream in this stage. On approaching the singularity, the disturbance enters the third stage in which the waves evolve over a faster streamwise length scale and non-equilibrium effects become important at leading order in the critical layer. In this stage, there is a continuing distortion of the normal distribution of the leading-order streamwise and spanwise disturbance velocities. The amplitude equation has the same nonlinear term as the one derived by Wu *et al.* (1993) for the interaction between a pair of

oblique Rayleigh instability waves. The solution to this amplitude equation is found to develop another singularity, which can be upstream or downstream of the one in the previous stage, depending on the obliqueness angle. In the vicinity of this new singularity, the flow is governed by the fully nonlinear three-dimensional inviscid triple-deck equations, i.e. long-wavelength Euler equations. The above nonlinear stages may characterize oblique-mode breakdown. It is worth noting that in the upper-branch-scaling regime, an initially linear disturbance does not evolve to a nonlinear stage with order-one changes in the mean flow and with the disturbance becoming neutral at very small magnitude (cf. Hall & Smith 1991).

Appendix C shows (*a*) that the evolution equations governing each of the nonlinear stages described above are all contained within the equation governing the evolution of a pair of oblique Rayleigh waves in the non-equilibrium viscous nonlinear critical layer regime, derived by Wu *et al.* (1993), and (*b*) that each of the former can be obtained as a limiting form of the latter. A uniformly valid solution for the oblique T-S wave evolution, from the linear growth through the non-equilibrium nonlinear stage will therefore be governed by the equation of Wu *et al.* (1993). The analysis shows that non-equilibrium critical layer effects ultimately control the development of initially linear instability waves even for a Blasius boundary layer, where the initial critical layer is dominated by viscous effects.

We have excluded any two-dimensional T-S wave in this study, and have considered the case where the imposed upstream disturbance consists only of a symmetric pair of oblique instability waves. While this is likely to be appropriate for K-type transition with pre-existing streamwise vortices, as in the original Klebanoff *et al.* (1962) experiment (see Goldstein & Wundrow 1995), it is more likely that the oblique waves will be amplified to nonlinear levels through a parametric resonance with a linearly growing plane wave in flows where subharmonic transition occurs, in which case the development may not follow the path as described above. However, the last two stages, namely the non-equilibrium critical-layer and the inviscid triple-deck regimes, appear to be 'attracting stages' for many types of initial disturbances, including the subharmonic resonant triad. For the resonant triad, the path leading to the non-equilibrium critical-layer regime depends on the magnitude of the oblique modes. In the case of exponentially small magnitude, a parametric resonance occurs first in the viscous-dominated critical-layer regime, causing super-exponential growth of the oblique modes, and the non-equilibrium stage follows immediately (Goldstein 1994; Wundrow, Hultgren & Goldstein 1994). For the case where the magnitude of oblique modes is algebraically small, the evolution equations governing the initial nonlinear development were given by Mankbadi *et al.* (1993) for a Blasius boundary layer, by Wu (1993) for a pressure gradient boundary layer, and a unified account of the general case was given by Lee (1994). The numerical solutions in these papers suggest, and it can be shown analytically, that the oblique wave amplitude eventually returns to its linear growth while phase oscillations are produced by the nonlinear self-interaction term (Goldstein 1996). The subsequent stages of the evolution are then exactly the same as in this paper. In particular, the wavelength shortening caused by the rapid phase oscillations leads to a WKBJ stage, whose breakdown leads to the non-equilibrium stage. The derivation of Appendix C suggests that the non-equilibrium critical layer equations given by Lee (1994) and Wu (1995) provide a uniformly valid description of the entire process, and the wave development in each nonlinear stage would be governed by appropriate limiting forms of the amplitude equations given in Wu (1995).

In a forthcoming paper, we show that a disturbance consisting of both two-

and three-dimensional T-S waves which are phase-locked but not of subharmonic-resonance form (cf. Wu & Stewart 1996) also evolves into the non-equilibrium critical-layer and the inviscid triple-deck stages. For both phase-locked and resonant-triad interactions, the disturbances in the final stage are governed by (6.4)–(6.6), subject to appropriate upstream conditions, which can be derived by studying the non-equilibrium critical layer regime for each case. For the resonant triad, a periodicity condition like (6.10) can be imposed, with T being the period of the oblique subharmonic modes. But a periodicity condition can no longer be imposed for the phase-locked disturbance, because the ratio of the frequencies of the planar and oblique modes is not a rational number in general. Nevertheless, the governing equations could be solved by a suitable spectral expansion in time.

It has been suggested (e.g. Kachanov *et al.* 1993) that the solution to the fully nonlinear system (6.4)–(6.6) may exhibit spikes. Such an outcome does not seems implausible since the solution contains the fundamental and all harmonics at leading order, so that a synchronization of their phases in a certain region of space could give rise to spikes (Kachanov 1994; Rist & Fasel 1995). The imposed periodicity condition is not expected to prevent the formation of spikes, since up to the double-spike stage the disturbance is still periodic in time (Kachanov 1994). However, the question of whether or not spikes appear is a complicated one because experiments show that it depends crucially on which type of disturbance is introduced; an argument based on the governing equations alone is not sufficient.

Recent experimental studies further suggest that spikes may be related to solitons (Borodulin & Kachanov 1990; Kachanov 1990, 1991). A theoretical effort has been made by Kachanov *et al.* (1993) to establish such a link. Their work is mainly concerned with two-dimensional disturbances, and is built on the fact that the two-dimensional version of (6.4)–(6.6) can be reduced to the so-called Benjamin–Ono equation (Zhuk & Ryzhov 1982; Smith & Burggraf 1985), which is known to possess a soliton type of solution. Unfortunately, for the fully three-dimensional system, such a simplification does not apply. Clearly, a two-dimensional theory is inadequate because spike formation is in reality a three-dimensional phenomenon. A firm theoretical confirmation of the soliton nature of spikes is yet to be achieved. In this respect, numerical studies of (6.4)–(6.10), with appropriate upstream conditions, may prove to be important.

The work of X.W. is supported by a Nuffield Foundation award. He would like to thank Dr S. J. Cowley and P. A. Stewart and Professor J. T. Stuart for helpful discussion.

Appendix A

The kernel function $K(\xi,\eta)$ is given by (3.85) of Wu *et al.* (1993). With a slight adjustment of notation, it can be written as

$$K(\xi,\eta\,|\,\Lambda)=\tilde{K}^{(0)}(\xi,\eta)(2\xi^3+\xi^2\eta)$$
$$+2\sin^2\theta\left\{\tilde{K}^{(0)}(\xi,\eta)\int_0^{\eta}[\xi^2+2\xi(\eta-\zeta)]\,\mathrm{e}^{-2\Lambda\zeta^3-3\Lambda\xi\zeta^2}\,\mathrm{d}\zeta\right.$$
$$\left.+\tilde{K}^{(0)}(\xi,\eta)\int_0^{\xi}[\zeta(2\eta+3\zeta)-\xi(\xi+2\eta+2\zeta)]\,\mathrm{e}^{-3\Lambda\xi\zeta^2}\,\mathrm{d}\zeta\right.$$

$$+2\tilde{K}^{(1)}(\xi,\eta)\int_0^{\xi}\eta\zeta[1+6\Lambda(\xi-\zeta)(\xi+\eta+\zeta)^2]\Pi_0(\xi,\eta,\zeta)\,\mathrm{d}\zeta$$
$$+\tilde{K}^{(1)}(\xi,\eta)\int_0^{\xi}[(\eta+\zeta)(\eta+3\zeta)-(\xi+\eta)(\xi+\eta+2\zeta)]\,\mathrm{e}^{-3\Lambda(\xi+\eta)(2\eta+\zeta)\zeta}\,\mathrm{d}\zeta\Big\}$$
$$+8\sin^4\theta\left\{\tilde{K}^{(0)}(\xi,\eta)\int_0^{\xi}\mathrm{d}\zeta\,\mathrm{e}^{-3\Lambda\xi\zeta^2}\int_0^{\eta+\zeta}(\upsilon-\eta-\zeta)[1+6\Lambda(\xi-\zeta)\zeta^2]\,\mathrm{e}^{-\Lambda(2\upsilon^3+3\xi\upsilon^2)}\,\mathrm{d}\upsilon\right.$$
$$+2\tilde{K}^{(1)}(\xi,\eta)\int_0^{\xi}\mathrm{d}\zeta\Pi_0(\xi,\eta,\zeta)\int_0^{\zeta}(\zeta-\upsilon)[1+6\Lambda(\xi-\zeta)(\xi+\eta+\zeta)^2]\,\mathrm{e}^{\Lambda(2\upsilon^3+3\eta\upsilon^2)}\,\mathrm{d}\upsilon$$
$$\left.+\tilde{K}^{(1)}(\xi,\eta)\int_0^{\xi}\mathrm{d}\zeta\,\mathrm{e}^{-3\Lambda(\xi+\eta)(2\eta+\zeta)\zeta}\int_0^{\zeta}(\upsilon-\zeta)[1+6\Lambda(\xi-\zeta)(\eta+\zeta)^2]\,\mathrm{e}^{-\Lambda[2\upsilon^3+3(\xi+\eta)\upsilon^2]}\,\mathrm{d}\upsilon\right\}, \tag{A 1}$$

where the auxiliary kernels $\tilde{K}^{(0)}$, $\tilde{K}^{(1)}$ and Π_0 are defined by

$$\tilde{K}^{(0)}(\xi,\eta)=\mathrm{e}^{-\Lambda(2\xi^3+3\xi^2\eta)}\,,\quad \tilde{K}^{(1)}(\xi,\eta)=\mathrm{e}^{-\Lambda[\xi^3+\eta^3+(\xi+\eta)^3]}\,, \tag{A 2}$$

$$\Pi_0(\xi,\eta,\zeta)=\mathrm{e}^{-\Lambda(4\zeta^3+6\xi\zeta^2+9\eta\zeta^2+6\xi\eta\zeta+6\eta^2\zeta)}\,. \tag{A 3}$$

Appendix B

We first consider the left-hand side of (5.11). It follows from differentiating (5.13) that

$$\tilde{A}'\to\left(-\tfrac{3}{4}\,\mathrm{i}\,\hat{\theta}_0(-\tilde{x})^{-1/4}-\tfrac{1}{4}\,\mathrm{i}\,\hat{\theta}_1(-\tilde{x})^{-3/4}\right)\tilde{A}_\infty(\tilde{x})\,\mathrm{e}^{\mathrm{i}\tilde{\Theta}_\infty}\,.$$
$$+\left(\tfrac{5}{8}\hat{a}_0(-\tilde{x})^{-13/8}+\tfrac{9}{8}\hat{a}_1(-\tilde{x})^{-17/8}\right)\mathrm{e}^{\mathrm{i}\tilde{\Theta}_\infty},\quad\text{as}\quad\tilde{x}\to-\infty, \tag{B 1}$$

where we have defined

$$\tilde{A}_\infty(\tilde{x})=\hat{a}_0(-\tilde{x})^{-5/8}+\hat{a}_1(-\tilde{x})^{-9/8},\quad\tilde{\Theta}_\infty(\tilde{x})=\hat{\theta}_0(-\tilde{x})^{3/4}+\hat{\theta}_1(-\tilde{x})^{1/4}.$$

In order to facilitate further calculations, the right-hand side of (5.11) is written as a sum of six terms as in Wu *et al.* (1993):

$$\mathrm{i}\,\tilde{\Upsilon}\Big\{N^{(0)}+N^{(1)}+2\sin^2\theta[N^{(2)}+N^{(3)}]+8\sin^4\theta N^{(4)}+N^{(5)}\Big\}\,, \tag{B 2}$$

where $N^{(j)}$ $(j=0,1,2,3,4,5)$ are defined in Appendix B of Wu *et al* (1993); see their (B2)–(B4). After substituting (5.13) into $N^{(0)}$ and $N^{(5)}$, and taking the limit $\tilde{x}\to-\infty$, we find that neither of these terms contributes to the dominant upstream balance.

For $N^{(1)}$, we perform the following substitution:

$$\xi\to(-\tilde{x})^{-1/2}\xi\,,\quad\eta\to(-\tilde{x})\eta\,, \tag{B 3}$$

and, upon taking the limit,

$$N^{(1)}\to\tfrac{1}{4}\pi^{1/2}(3s)^{-3/2}I_0\hat{a}_0^2(-\tilde{x})^{-3/4}\tilde{A}_\infty(\tilde{x})\,\mathrm{e}^{\mathrm{i}\tilde{\Theta}_\infty}\,, \tag{B 4}$$

with I_0 given by (4.86). The function $N^{(3)}$ can be split into the three terms defined by (B16) of Wu *et al.* (1993), and only the second term, which is similar to $N^{(1)}$, contributes to the upstream balance with

$$N^{(3)}\to-\tfrac{1}{4}\pi^{1/2}(3s)^{-3/2}I_0\hat{a}_0^2(-\tilde{x})^{-3/4}\tilde{A}_\infty(\tilde{x})\,\mathrm{e}^{\mathrm{i}\tilde{\Theta}_\infty}\,. \tag{B 5}$$

In the limit $\tilde{x} \to -\infty$, the leading-order contribution to the right-hand side of (5.11) comes from $N^{(2)}$ and $N^{(4)}$, which we now consider. For convenience, we first define

$$\begin{aligned} G(\tilde{x};\xi,\eta)=&\Big[(-\tilde{x}+\xi)(-\tilde{x}+\xi+\eta)(-\tilde{x}+2\xi+\eta)\Big]^{-5/8} \\ &\times\Big(\hat{a}_0+\hat{a}_1(-\tilde{x}+\xi)^{-1/2}\Big)\Big(\hat{a}_0+\hat{a}_1(-\tilde{x}+\xi+\eta)^{-1/2}\Big)\Big(\hat{a}_0+\hat{a}_1(-\tilde{x}+2\xi+\eta)^{-1/2}\Big) \\ &\times\exp\Big\{\mathrm{i}\,\hat{\theta}_0[(-\tilde{x}+\xi)^{3/4}+(-\tilde{x}+\xi+\eta)^{3/4}-(-\tilde{x}+2\xi+\eta)^{3/4}] \\ &+\mathrm{i}\,\hat{\theta}_1[(-\tilde{x}+\xi)^{1/4}+(-\tilde{x}+\xi+\eta)^{1/4}-(-\tilde{x}+2\xi+\eta)^{1/4}]\Big\}\ . \end{aligned} \tag{B 6}$$

It follows from the substitution of (5.13) into $N^{(2)}$ ((B14) in Wu *et al.* 1993) that

$$N^{(2)} \to \int_0^{+\infty}\int_0^{+\infty}\int_0^{+\infty}(2\xi\eta)\,\mathrm{e}^{-2s\xi^3-3s\xi^2(\eta+\zeta)-2s\zeta^3-3s\xi\zeta^2}\,G(\tilde{x};\xi,\eta+\zeta)\,\mathrm{d}\xi\,\mathrm{d}\eta\,\mathrm{d}\zeta\ . \tag{B 7}$$

Integrating by parts with respect to ξ, we obtain

$$\begin{aligned} N^{(2)}=&(3s)^{-1}\left\{\tilde{A}_\infty\,\mathrm{e}^{\mathrm{i}\tilde{\Theta}_\infty}\int_0^{+\infty}\int_0^{+\infty}(-\tilde{x}+\eta+\zeta)^{-5/4}\Big[\hat{a}_0+\hat{a}_1(-\tilde{x}+\eta+\zeta)^{-1/2}\Big]^2\,\mathrm{e}^{-2s\zeta^3}\,\mathrm{d}\eta\,\mathrm{d}\zeta\right. \\ &+\frac{3}{4}\,\mathrm{i}\,\hat{\theta}_0\int_0^{+\infty}\int_0^{+\infty}\int_0^{+\infty}\Big[(-\tilde{x}+\xi)^{-1/4}+(-\tilde{x}+\xi+\eta+\zeta)^{-1/4}-2(-\tilde{x}+2\xi+\eta+\zeta)^{-1/4}\Big] \\ &\qquad\mathrm{e}^{-2s\xi^3-3s\xi^2(\eta+\zeta)-2s\zeta^3-3s\xi\zeta^2}\,G(\tilde{x};\xi,\eta+\zeta)\,\mathrm{d}\xi\,\mathrm{d}\eta\,\mathrm{d}\zeta \\ &+\frac{1}{4}\,\mathrm{i}\,\hat{\theta}_1\int_0^{+\infty}\int_0^{+\infty}\int_0^{+\infty}\Big[(-\tilde{x}+\xi)^{-3/4}+(-\tilde{x}+\xi+\eta+\zeta)^{-3/4}-2(-\tilde{x}+2\xi+\eta+\zeta)^{-3/4}\Big] \\ &\qquad\mathrm{e}^{-2s\xi^3-3s\xi^2(\eta+\zeta)-2s\zeta^3-3s\xi\zeta^2}\,G(\tilde{x};\xi,\eta+\zeta)\,\mathrm{d}\xi\,\mathrm{d}\eta\,\mathrm{d}\zeta \\ &\left.+(-3s)\int_0^{+\infty}\int_0^{+\infty}\int_0^{+\infty}\zeta^2\,\mathrm{e}^{-2s\xi^3-3s\xi^2(\eta+\zeta)-2s\zeta^3-3s\xi\zeta^2}\,G(\tilde{x};\xi,\eta+\zeta)\,\mathrm{d}\xi\,\mathrm{d}\eta\,\mathrm{d}\zeta\right\} \\ &+\dots\ , \end{aligned} \tag{B 8}$$

where we have ignored the terms whose asymptotes are much smaller than those in which we are interested. After making the substitution (B 3) and taking the limit $\tilde{x} \to -\infty$, we find that

$$\begin{aligned} N^{(2)}\to&\left\{8\Lambda\hat{a}_0^2(-\tilde{x})^{-1/4}+\left(\tfrac{16}{3}\Lambda\hat{a}_0\hat{a}_1-\tfrac{1}{4}\pi^{1/2}4(3s)^{-3/2}I_0\hat{a}_0^2\right)(-\tilde{x})^{-3/4}\right\}\tilde{A}_\infty\,\mathrm{e}^{\mathrm{i}\tilde{\Theta}_\infty} \\ &+\tfrac{1}{4}\pi^{1/2}\,\mathrm{i}(3s)^{-1/2}\Lambda\hat{a}_0^2\left\{3J_0\hat{a}_0\hat{\theta}_0(-\tilde{x})^{-13/8}+\Big(\Lambda_0\hat{a}_0\hat{\theta}_1+3K_0\hat{\theta}_0\hat{a}_1\Big)(-\tilde{x})^{-17/8}\right\}\mathrm{e}^{\mathrm{i}\tilde{\Theta}_\infty}\ , \end{aligned} \tag{B 9}$$

where $\Lambda = \frac{1}{9}(-2s)^{-4/3}\Gamma(1/3)$, while J_0, I_0, Λ_0 and K_0 are defined by (4.80) and (4.86)–(4.88) respectively.

The function $N^{(4)}$ is given by (B18) of Wu *et al.* (1993), of which only the third term is significant, yielding

$$N^{(4)} \to -\int_0^{+\infty}\int_0^{+\infty}\int_0^{+\infty}\xi\eta\,\mathrm{e}^{-2s\xi^3-3s\xi^2(\eta+\upsilon)-s(2\upsilon^3+3\xi\upsilon^2)}\,G(\tilde{x};\xi,\eta+\upsilon)\,\mathrm{d}\xi\,\mathrm{d}\eta\,\mathrm{d}\upsilon, \tag{B 10}$$

which is the same as (B.7) except for a factor of $-\frac{1}{2}$. Combining this with (B 4), (B 5),

(B 9) and (B 2), we conclude that as $\tilde{x} \to -\infty$, the right-hand side of (5.11) tends to

$$\begin{aligned}
&\mathrm{i}\,\tilde{\Upsilon}\Big\{ \tfrac{16}{9}\sin^2\theta\cos 2\theta(2s)^{-4/3}\Gamma\left(\tfrac{1}{3}\right)\hat{a}_0^2(-\tilde{x})^{-1/4} \\
&+\Big(\tfrac{32}{27}\sin^2\theta\cos 2\theta(2s)^{-4/3}\Gamma\left(\tfrac{1}{3}\right)\hat{a}_0\hat{a}_1+\tfrac{1}{4}\pi^{1/2}\cos^2 2\theta(3s)^{-3/2}I_0\hat{a}_0^2\Big)(-\tilde{x})^{-3/4}\Big\}\tilde{A}_\infty\,\mathrm{e}^{\mathrm{i}\tilde{\Theta}_\infty} \\
&-\tfrac{1}{18}\pi^{1/2}\tilde{\Upsilon}\sin^2\theta\cos 2\theta(2s)^{-4/3}(3s)^{-1/2}\Gamma\left(\tfrac{1}{3}\right)\hat{a}_0^2 \\
&\quad\Big\{3J_0\hat{a}_0\hat{\theta}_0(-\tilde{x})^{-13/8}+\Big(\Lambda_0\hat{a}_0\hat{\theta}_1+3K_0\hat{\theta}_0\hat{a}_1\Big)(-\tilde{x})^{-17/8}\Big\}\,\mathrm{e}^{\mathrm{i}\,\tilde{\Theta}_\infty}\,. \qquad \text{(B 11)}
\end{aligned}$$

Equating the coefficients of like powers in (B 1) and (B 11) gives

$$-\tfrac{3}{4}\hat{\theta}_0=\tfrac{16}{9}\Gamma\left(\tfrac{1}{3}\right)\tilde{\Upsilon}\sin^2\theta\cos 2\theta(2s)^{-4/3}|\hat{a}_0|^2\,, \qquad \text{(B 12)}$$

$$\tfrac{5}{8}=-\tfrac{1}{6}\pi^{1/2}\Gamma\left(\tfrac{1}{3}\right)\tilde{\Upsilon}\sin^2\theta\cos 2\theta(3s)^{-1/2}(2s)^{-4/3}J_0\hat{\theta}_0|\hat{a}_0|^2\,; \qquad \text{(B 13)}$$

$$-\tfrac{1}{4}\hat{\theta}_1=\tfrac{32}{27}\tilde{\Upsilon}\sin^2\theta\cos 2\theta(2s)^{-4/3}\Gamma\left(\tfrac{1}{3}\right)\hat{a}_0\hat{a}_1-\tfrac{1}{4}\pi^{1/2}\tilde{\Upsilon}\cos^2 2\theta(3s)^{-3/2}I_0\hat{a}_0^2\,, \qquad \text{(B 14)}$$

$$\tfrac{9}{8}\hat{a}_1=\tfrac{1}{18}\pi^{1/2}\tilde{\Upsilon}\sin^2\theta\cos 2\theta(2s)^{-4/3}(3s)^{-1/2}\Gamma\left(\tfrac{1}{3}\right)\hat{a}_0^2(\Lambda_0\hat{a}_0\hat{\theta}_1+3K_0\hat{\theta}_0\hat{a}_1)\,. \qquad \text{(B 15)}$$

It is noted that (B 12) and (B 13) are equivalent to (4.79) and (4.82), while (B 14) and (B 15) are equivalent to (4.84) and (4.85). This shows that for the upstream condition (5.13), both sides of (5.11) indeed have the same asymptotic behaviour as $\tilde{x} \to -\infty$.

Appendix C

In this appendix we show that the evolution equations derived in §§3–5, which govern the three weakly nonlinear stages through which an initially linear pair of oblique T-S waves evolve, are all contained within the nonlinear non-equilibrium viscous critical layer amplitude equation, and how the former equations may be derived as limiting forms of the latter.

The nonlinear non-equilibrium viscous critical layer amplitude equation may be written as (Wu *et al.* 1993)

$$\frac{\mathrm{d}\bar{A}}{\mathrm{d}\bar{\xi}}=\bar{\kappa}\bar{A}-\mathrm{i}\,\bar{\gamma}\int_{-\infty}^{\bar{\xi}}\int_{-\infty}^{\bar{\xi}_1}K(\bar{\xi}-\bar{\xi}_1,\bar{\xi}_1-\bar{\xi}_2|\Lambda)\bar{A}(\bar{\xi}_1)\bar{A}(\bar{\xi}_2)\bar{A}^*(\bar{\xi}_1+\bar{\xi}_2-\bar{\xi})\,\mathrm{d}\bar{\xi}_2\,\mathrm{d}\bar{\xi}_1\,, \qquad \text{(C 1)}$$

where $\bar{\xi}$ is the long streamwise variable over which the amplitude evolves, Λ is the viscous parameter and the coefficients $\bar{\kappa}$ and $\bar{\gamma}$, which in general can be complex constants, are purely real in the long-wavelength limit of interest here. The kernel function K is that given by Wu *et al.* (1993) and is reproduced here in Appendix A. From the upper-branch scaling and definition of the viscous parameter we have that $\Lambda=\sigma^{-3/2}$.

The amplitude in the first, wavelength-shortening, nonlinear stage is governed by the highly viscous limit (i.e. $\Lambda \to \infty$) of (C 1). This limit was worked out by Wu *et al.* (1993). Substituting

$$x_1=\sigma^{1/2}\bar{\xi}, \qquad A=\sigma^{1/2}\bar{A}, \qquad \kappa=\sigma^{-1/2}\bar{\kappa}, \qquad \text{(C 2)}$$

into (C 1) and using the results for the highly viscous limit of the integral nonlinear term given in appendix B of Wu *et al.* (1993) we obtain

$$\frac{\mathrm{d}A}{\mathrm{d}x_1} = \kappa A - \frac{\mathrm{i}\,\bar{\gamma}}{(\alpha_0\lambda)^{8/3}} \left(\tfrac{2}{3}\right)^{2/3} \Gamma\left(\tfrac{1}{3}\right) \sin^2\theta \cos 2\theta A \int_0^\infty |A(x_1-\zeta)|^2\,\mathrm{d}\zeta \tag{C 3}$$

which agrees with (3.2) provided we put

$$\bar{\gamma} = -\frac{\Upsilon(\alpha_0\lambda)^{8/3}}{\left(\tfrac{2}{3}\right)^{2/3}\Gamma\left(\tfrac{1}{3}\right)\sin^2\theta\cos 2\theta}. \tag{C 4}$$

In the WKBJ stage of evolution the solution is of the form

$$\bar{A} = \sigma^{-7/8}\hat{A}(\hat{x})\,\mathrm{e}^{\mathrm{i}\sigma^{-3/4}\hat{\Theta}(\hat{x})}, \tag{C 5}$$

where

$$\hat{x} = \sigma^{1/2}\bar{\xi} - \frac{1}{\kappa}\ln\sigma^{-3/8} + \hat{x}_0 \tag{C 6}$$

is order one. Substituting (C 5) and (C 6) into (C 1), we obtain

$$\mathrm{i}\frac{\mathrm{d}\hat{\Theta}}{\mathrm{d}\hat{x}} = \sigma^{3/4}\left[\kappa - \frac{\mathrm{d}}{\mathrm{d}\hat{x}}\ln\hat{A}\right] - \frac{\mathrm{i}\,\bar{\gamma}}{\hat{A}}\hat{N}(\hat{x}), \tag{C 7}$$

where

$$\hat{N}(\hat{x}) = \sigma^{-4}\int_{-\infty}^{\hat{x}}\int_{-\infty}^{\hat{x}_1} K(\hat{x}-\hat{x}_1,\hat{x}_1-\hat{x}_2|\Lambda\sigma^{-3/2})\hat{A}(\hat{x}_1)\hat{A}(\hat{x}_2)\hat{A}^*(\hat{x}_1+\hat{x}_2-\hat{x}) \times \mathrm{e}^{\mathrm{i}\sigma^{-3/4}[\hat{\Theta}(\hat{x}_1)+\hat{\Theta}(\hat{x}_2)-\hat{\Theta}(\hat{x}_1+\hat{x}_2-\hat{x})-\hat{\Theta}(\hat{x})]}\,\mathrm{d}\hat{x}_2\,\mathrm{d}\hat{x}_1\,. \tag{C 8}$$

The asymptotic expansion of $\hat{N}$ can be derived following the procedure used by Wu *et al.* (1993) to derive the viscous limit. To the order of approximation needed here only the terms analogous to $N^{(2)}$ and $N^{(4)}$ (see their Appendix B) of their derivation contribute to the evolution equations in this stage, with the critical difference being that here higher-order contributions from these terms must be retained. First introducing $\hat{t}_1 = \hat{x} - \hat{x}_1$ and $\hat{\eta} = \hat{x}_1 - \hat{x}_2$ into (C 8) and then, following the general procedure in Wu *et al.* (1993), substituting

$$\bar{t}_1 = \sigma^{-3/4}(\alpha_0\lambda)\hat{t}_1;\quad \bar{t}_3 = \sigma^{-1}(\alpha_0\lambda)^{2/3}\hat{t}_3;\quad \bar{t}_4 = \sigma^{-1}(\alpha_0\lambda)^{2/3}\hat{t}_4, \tag{C 9}$$

into the relevant terms, we find the expansion of $\hat{N}$ to the required order of approximation to be

$$\begin{aligned}\hat{N}\sim{}&\frac{\left(\tfrac{2}{3}\right)^{2/3}\Gamma\left(\tfrac{1}{3}\right)}{(\alpha_0\lambda)^{8/3}}\sin^2\theta\cos 2\theta\hat{A}\int_0^\infty|\hat{A}(\hat{x}-\hat{\eta})|^2\,\mathrm{d}\hat{\eta}\\ &+\frac{\sigma^{1/2}}{(\alpha_0\lambda)^3}\frac{\pi^{1/2}}{8}(1+\cos\theta)\,\hat{A}\int_0^\infty\frac{|\hat{A}(\hat{x}-\hat{\eta})|^2}{\hat{\eta}^{1/2}}\,\mathrm{d}\hat{\eta}\\ &-\frac{\mathrm{i}\,\sigma^{3/4}}{(\alpha_0\lambda)^{11/3}}\frac{\pi^{1/2}}{2}\left(\tfrac{2}{3}\right)^{2/3}\Gamma\left(\tfrac{1}{3}\right)\sin^2\theta\cos 2\theta\hat{A}\int_0^\infty\frac{|\hat{A}(\hat{x}-\hat{\eta})|^2}{\hat{\eta}^{1/2}}\left[\hat{\Theta}'(\hat{x})-\hat{\Theta}'(\hat{x}-\hat{\eta})\right]\mathrm{d}\hat{\eta}.\end{aligned} \tag{C 10}$$

Substituting this into (C 7) shows that the equations for the phase and amplitude

in the WKBJ region are

$$\frac{\mathrm{d}\hat{\Theta}}{\mathrm{d}\hat{x}}=-\frac{\bar{\gamma}}{(\alpha_0\lambda)^{8/3}}\left(\tfrac{2}{3}\right)^{2/3}\Gamma\left(\tfrac{1}{3}\right)\sin^2\theta\cos 2\theta\int_0^\infty|\hat{A}(\hat{x}-\hat{\eta})|^2\,\mathrm{d}\hat{\eta}$$
$$-\frac{\bar{\gamma}\sigma^{1/2}}{(\alpha_0\lambda)^3}\frac{\pi^{1/2}}{8}(1+\cos\theta)\int_0^\infty\frac{|\hat{A}(\hat{x}-\hat{\eta})|^2}{\hat{\eta}^{1/2}}\,\mathrm{d}\hat{\eta}, \tag{C 11}$$

and

$$\frac{\mathrm{d}\hat{A}}{\mathrm{d}\hat{x}}=\kappa\hat{A}-\frac{\bar{\gamma}}{(\alpha_0\lambda)^{11/3}}\frac{\pi^{1/2}}{2}\left(\tfrac{2}{3}\right)^{2/3}\Gamma\left(\tfrac{1}{3}\right)\sin^2\theta\cos 2\theta\hat{A}$$
$$\times\int_0^\infty\frac{|\hat{A}(\hat{x}-\hat{\eta})|^2}{\hat{\eta}^{1/2}}\left[\hat{\Theta}'(\hat{x})-\hat{\Theta}'(\hat{x}-\hat{\eta})\right]\mathrm{d}\hat{\eta}, \tag{C 12}$$

which, upon using (C 4), give (4.69) and (4.70), respectively. As shown in §4 the leading-order equations for the amplitude and phase functions can be combined to arrive at a single equation for the modulus which is the same as (4.73).

In the final weakly nonlinear stage the disturbance evolves with the streamwise variable

$$\tilde{x}=(\hat{x}_c-\hat{x})/\sigma, \tag{C 13}$$

and the scaled amplitude function

$$\tilde{A}=\sigma^{3/2}\bar{A}, \tag{C 14}$$

of order one. Substituting these into (C 1) shows that the linear growth term is now negligible to leading order due to the very fast spatial evolution in this stage. The effective viscous parameter is now of order one so that the full non-equilibrium nonlinear term is retained at leading order and the amplitude equation is

$$\frac{\mathrm{d}\tilde{A}}{\mathrm{d}\tilde{x}}=-\mathrm{i}\,\bar{\gamma}\int_{-\infty}^{\tilde{x}}\int_{-\infty}^{\tilde{x}_1}K(\tilde{x}-\tilde{x}_1,\tilde{x}_1-\tilde{x}_2|\Lambda\sigma^{3/2})\tilde{A}(\tilde{x}_1)\tilde{A}(\tilde{x}_2)\tilde{A}^*(\tilde{x}_1+\tilde{x}_2-\tilde{x})\,\mathrm{d}\tilde{x}_2\,\mathrm{d}\tilde{x}_1. \tag{C 15}$$

Non-equilibrium critical layer effects have a leading-order influence on the amplitude evolution in this stage with the result that the solution develops the finite-distance singularity originally derived by Goldstein & Choi (1989).

The analysis in this Appendix shows that a solution for the oblique T-S wave amplitude, uniformly valid throughout the linear and weakly nonlinear regimes, is governed by the non-equilibrium viscous nonlinear critical layer equation derived by Wu *et al.* (1993).

REFERENCES

Brown, S. N. & Smith, F. T. 1996 On wave/vortex interactions. Part 1. Nonsymmetrical input and cross-flow in boundary layers. *J. Fluid Mech.* **307**, 101–134.

Blackaby, N. D. 1994 Tollmien-Schlichting/vortex interactions in compressible boundary layer flows. *IMA J. Appl. Maths* **53**, 191–214.

Bodonyi, R. J. & Smith, F. T. 1981 The upper-branch stability of the Blasius boundary layer, including non-parallel flow effects. *Proc. R. Soc. Lond.* A **375**, 65–92.

Borodulin, V. I. & Kachanov, Y. S. 1988 Role of the mechanism of local secondary instability in K-breakdown of boundary layer. *Proc. Siberian Div, USSR Acad. Sci. Tech. Sci.* **18**, 65–77. See also *Sov. J. Appl. Phys.* **3**(2), 70–81, 1989.

Chang, C.-L. & Malik, M. R. 1994 Oblique-mode breakdown and secondary instability in supersonic boundary layers. *J. Fluid Mech.* **273**, 323–360.

Corke, T. C. & Mangano, R. A. 1989 Resonant growth of three-dimensional modes in transitioning Blasius boundary layers. *J Fluid Mech.* **209**, 93–150.

Cowley, S. J., Van Dommelen, L. & Lam, L. L. 1991 On the use of Lagrangian variables in descriptions of unsteady boundary–layer separation. *Phil. Trans. R. Soc. Lond.* A **333**, 343–378.

Cowley, S. J. & Wu, X. 1994 Asymptotic approaches to transition modelling. In *Progress in Transition Modelling*, AGARD Report 793, Chapter 3, 1–38.

Davis, D. A. R. & Smith, F. T. 1994 Influence of cross-flow on nonlinear Tollmien-Schlichting wave/vortex interaction. *Proc. R. Soc. Lond.* A **446**, 319–340.

Fasel, H., Thumm, A. & Bestek, H. 1993 Direct numerical simulation of transition in supersonic boundary layers: oblique breakdown. In *Transition and Turbulent Compressible Flows.* ASME FED vol. 151 (ed. L. D. Kral & T. A. Zang), pp. 77–92.

Fischer, M. C. & Weinstein, L. M. 1972 Cone transitional boundary-layer structure at $Me = 14$. *AIAA. J.* **10**, 699–701.

Goldstein, M. E. 1994 Nonlinear interactions between oblique instability waves on nearly parallel shear flows. *Phys. Fluids* A **6**, 724–735.

Goldstein, M. E. 1996 The role of nonlinear critical layers in transition to turbulence in boundary layers. *AIAA Paper* 2122.

Goldstein, M. E. & Choi, S.-W. 1989 Nonlinear evolution of interacting oblique waves on two-dimensional shear layers. *J. Fluid Mech.* **207**, 97–120, and Corrigendum, *J. Fluid Mech.* **216**, 1990, 659–663.

Goldstein, M. E. & Durbin, P. A. 1986 Nonlinear critical layers eliminate the upper branch of spatially growing Tollmien-Schlichting waves. *Phys. Fluids* **29**, 2344–2345.

Goldstein, M. E. & Lee, S. S. 1992 Fully coupled resonant-triad interaction in an adverse-pressure-gradient boundary layer. *J. Fluid Mech.* **245**, 523–551.

Goldstein, M. E. & Wundrow, D. W. 1995 Interaction of oblique instability waves with weak streamwise vortices. *J. Fluid Mech.* **284**, 377–407.

Hall, P. & Smith, F. T. 1989 Nonlinear Tollmien-Schlichting/vortex interaction in boundary layers. *Eur. J. Mech.* B **8**, 179–205.

Hall, P. & Smith, F. T. 1991 On strongly nonlinear vortex/wave interactions in boundary-layer transition. *J. Fluid Mech.* **227**, 641–666.

Healey, J. J. 1994 On the neutral curve of the flat-plate boundary layer: comparison between experiment, Orr-Sommerfeld theory and asymptotic theory. *J. Fluid Mech.* **288**, 59–83.

Hickernell, F. J. 1984 Time-dependent critical layers in shear flows on the beta-plane. *J. Fluid Mech.* **142**, 431–449.

Joslin, R. D., Streett, C. L. & Chang, C.-L. 1993 Spatial direct numerical simulation of boundary-layer mechanisms: validation of PSE theory. *Theor. Comput. Fluid Dyn.* **4**, 171–288.

Kachanov, Y. S. 1990 Secondary and resonant instabilities of boundary layers, wave-resonant concept of a breakdown and its substantiation. In *Laminar–Turbulent Transition* (ed. A. Arnal & R. Michel), pp. 65–80. Springer.

Kachanov, Y. S. 1991 The mechanisms of formation and breakdown of soliton–like coherent structures in a boundary layer. In *Advances in Turbulence*, vol. 3 (ed. A.V. Johannson & P.H. Alfredsson), pp. 42-51. Springer.

Kachanov, Y. S. 1994 Physical mechanisms of laminar-boundary-layer transition. *Ann. Rev. Fluid Mech.* **26**, 411–482.

Kachanov, Y. S. & Levchenko, V. Ya. 1984 The resonant interaction of disturbances at laminar-turbulent transition in a boundary layer. *J. Fluid Mech.* **138**, 209–247.

Kachanov, Y. S., Ryzhov, O. S. & Smith, F. T. 1993 Formation of solitons in transitional boundary layer: theory and experiments. *J. Fluid Mech.* **251**, 251–297.

Klebanoff, P. S., Tidstrom, K. D. & Sargent, L. M. 1962 The three-dimensional nature of boundary layer instability. *J. Fluid Mech.* **12**, 1–34.

Lee, S. S. 1994 Critical-layer analysis of fully coupled resonant-triad interaction in a boundary layer. Submitted to *J. Fluid Mech.*

Leib, S. J. & Lee, S. S. 1995 Nonlinear evolution of a pair of oblique instability waves in a supersonic boundary layer. *J. Fluid Mech.* **282**, 339–371.

Mankbadi, R. R., Wu, X. & Lee, S. S. 1993 A critical-layer analysis of the resonant triad in Blasius boundary-layer transition: nonlinear interactions. *J. Fluid Mech.* **256**, 85–106.

Pruett, C. D. & Chang, C.-L. 1995 Spatial direct numerical simulation of of high-speed boundary-layer flows. Part II: transition on a cone in Mach 8 flow. *Theor. Comput. Fluid Dyn.* **7**, 397–424.

Pruett, C. D. & Zang, T. A. 1992 Direct numerical simulation of laminar breakdown in high-speed axisymmetric boundary layers. *Theor. Comput. Fluid Dyn.* **3**, 345–367.

Reid, W. H. 1965 The stability of parallel flows. In *Basic Developments in Fluid Dynamics* (ed. M. Holt), pp. 249–308. Academic.

Rist, U. & Fasel, H. 1995 Direct numerical simulation of controlled transition in a flat-plate boundary layer. *J. Fluid Mech.* **298**, 211–248.

Schmid, P. J. & Henningson, D. S. 1992*a* Channel flow transition induced by a pair of oblique waves. In *Stability, Transition and Turbulence* (ed. M. Y. Hussaini, A. Kumar & C. L. Streett), pp. 356–366. Springer.

Schmid, P. J. & Henningson, D. S. 1992*b* A new mechanism of rapid transition involving a pair of oblique waves. *Phys. Fluids* A **419**, 1986–1989.

Smith, F. T. & Blennerhassett, P. 1992 Nonlinear interaction of oblique three-dimensional Tollmien-Schlichting waves and longitudinal vortices, in channel flows and boundary layers. *Proc. R. Soc. Lond.* A **436**, 585–602.

Smith, F. T. & Bodonyi, R. J. 1982 Nonlinear critical layers and their development in streaming-flow stability. *J. Fluid Mech.* **118**, 165–185.

Smith F. T., Brown S. N. & Brown P. G. 1993 Initiation of three-dimensional nonlinear transition paths from an inflectional profile. *Eur. J. Mech.* B **12**, 447–473.

Smith, F. T. & Burggraf, O. R. 1985 On the development of large-sized short-scaled disturbances in boundary layers. *Proc. R. Soc. Lond.* A **399**, 25–55.

Smith, F. T. & Stewart, P. A. 1987 The resonant-triad nonlinear interaction in boundary-layer transition. *J. Fluid Mech.* **179**, 227–252.

Stuart, J. T. 1960 On the nonlinear mechanisms of wave disturbances in stable and unstable parallel flows. Part 1. *J. Fluid Mech.* **9**, 353–370.

Wu, X. 1993 On critical-layer and diffusion-layer nonlinearity in the three-dimensional stage of boundary-layer transition. *Proc. R. Soc. Lond.* A **443**, 95–106.

Wu, X. 1995 Viscous effects on fully coupled resonant-triad interactions: an analytical approach. *J. Fluid Mech.* **292**, 377–407.

Wu, X., Lee, S. S. & Cowley, S. J. 1993 On the weakly nonlinear three-dimensional instability of shear flows to pairs of oblique waves: the Stokes layer as a paradigm. *J. Fluid Mech.* **253**, 681–721.

Wu, X. & Stewart, P. A. 1996 Interaction of phase-locked modes: a new mechanism for the rapid growth of three-dimensional disturbances. *J. Fluid Mech.* **316**, 335–372.

Wu, X., Stewart, P. A. & Cowley, S. J. 1996 On the weakly development of Tollmien-Schlichting wave-trains in boundary layers. *J. Fluid Mech.* **323**, 133–171.

Wundrow, D. W. & Goldstein, M. E. 1995 Nonlinear instability of a uni-directional transversely sheared mean flow. *NASA TM* 106779.

Wundrow, D. W., Hultgren, L. S. & Goldstein, M. E. 1994 Interaction of oblique instability waves with a nonlinear plane wave. *J. Fluid Mech.* **264**, 343–372.

Zhuk, V. I. & Ryzhov, O. S. 1982 On locally-inviscid disturbances in boundary layer with self-induced pressure. *Dokl. Akad. Nauk. SSSR* **263**(1), 56–69. See also *Sov. Phys. Dokl.* **27**(3), 177–179.

Zhuk, V. I. & Ryzhov, O. S. 1989 On 3d inviscid disturbances inducing their own pressure gradient in a boundary layer. *Dokl. Akad. Nauk. SSSR* **301**(1), 52–56. See also *Sov. Phys. Dokl.* **34**(11), 949–951.